# *Biological activity of a set of new copper(II) complexes: toward understanding structure-reactivity correlations*

By

Chelsea L. Aitken

**********

Submitted in partial fulfillment

Of the requirements for

Honors in the Department of Biochemistry

UNION COLLEGE

June, 2014

**ABSTRACT**

AITKEN,CHELSEA *Biological activity of a set of new copper(II) complexes: toward understanding structure-reactivity correlations*

ADVISOR: Professor Laurie A. Tyler

Cisplatin, carboplatin and oxaliplatin are all platinum-containing complexes that have been approved for use as chemotherapy drugs. The success of these complexes as well as their downfalls have sparked interest into alternative transition metal based compounds as potential chemotherapeutic agents. The use of platinum based complexes in cancer treatment has faced complications including cytotoxicity and drug resistance. The use of copper(II) as an alternative metal center is of specific interest because of bioavailability and elevated concentrations of this metal ion within tumor cells. Three copper complexes that utilize a nitrogen based ligand system, two of which contain a thiazole moiety have been synthesized and characterized. The biological activity and potential cytotoxicity of these complexes was measured on the basis of nuclease activity, DNA binding, and interaction with BSA. These characteristics were determined by quantitative analysis of studies using ethidium bromide, gel electrophoresis, and UV-Vis spectroscopy. It has been shown that all of these complexes exhibit concentration dependent nuclease activity utilizing a mechanism dependent on reactive oxygen species. Here, comparisons between the activity of these newly synthesized compounds and those previously studied are presented to aid in developing a correlation between ligand structure and complex activity.

***Table of Contents***

Chelse
Delete
Chelse
Delete
Chelse
Delete

## 1. Introduction

The American Cancer Society estimated that in the U.S. 1,638,910 new cases of cancer were diagnosed in 2012 alone and 577,190 cancer related deaths occurred.[1] These numbers demonstrate the prevalence of cancer and highlight the great impact it has on our lives. Most of our lives have been touched by cancer in some way, whether as the patient, a family member, or a friend. Research in this field is ongoing and of extreme importance.

In humans, all the cells within a tumor are believed to originate from a single cell that was converted from a normal cell to a cancerous cell. This type of cancer origination is named monoclonal, the other possibility (polyclonal origination) has not been observed in humans.[2] The next question then becomes how does a cell convert from a normal cell to a cancerous one. Cancer occurs once multiple mutations have been sustained and propagated. Often these mutations are specific to genes responsible for regulating cell cycle control, allowing the cancerous cells to proceed through the cell cycle and produce progeny despite sustained mutations.[2] Typically a single mutation, particularly in an essential gene, will promote a cell to undergo programmed cell death preventing the spread of that mutation to subsequent generations of cells. However, some mutations are not repaired in time and in many cases with pre-cancerous mutations the mutated gene actually allows the daughter cells to be more susceptible to sustaining subsequent mutations because the initially mutated gene was involved in a pathway responsible for cell division control or DNA damage monitoring.[2,3] Cancer is not really a single disease, but rather many diseases with one unifying factor, the ability of cells to proliferate

without regulation.[3] A tumor is a mass of these mutated cells that are dividing without regulation and the tumor is considered malignant once the cancerous cells begin to invade tissues outside of their native region in the body. Cancers can be divided into four predominant types: carcinomas, sarcomas, leukemia, and lymphoma.[3]

*1.1 Inducing programmed cell death in cancerous cells*

Apoptosis is a form of highly controlled internally initiated cell death. Various factors, intracellular and extracellular, can be responsible for triggering this response in cells. This type of cell death is advantageous because the cell shrinks and then breaks into membrane enclosed fragments, which can later be digested without any harm to surrounding cells.[4,5] There are three circumstances under which apoptosis typically occur. The first involves apoptosis initiated by environmental factors, such as limited physical space or cellular resources this is termed *utilitarian cell suicide*, because a perfectly healthy cell undergoes cell death for the overall benefit of the surrounding cellular population.[4] This is specifically useful during development. Apoptosis can also be triggered in cells once they have reached or surpassed their cellular life expectancy; this is called *senescent cell suicide.*[4] Finally, the situation that triggers apoptosis that is most relevant to our discussion of cancer and cancer treatments, involves the initiation of apoptosis due to cellular damage. Damage to DNA, cellular membranes, or other vital cellular components induces the cell to initiate programmed cell death rather than risk incorrectly repairing the damage and propagating it to subsequent generations.[4]

There is a strong correlation between genes involved in the apoptotic pathway and cancer. Tumor suppressor genes are typically involved in controlling proliferation and do so by acting as signals in control pathways including apoptosis, cell cycle, and DNA repair. Genes are considered tumor suppressors not only because they are essential in these types of pathways, but also because their absence has been shown to promote cancer.[5] p53 is one of the quintessential tumor suppressor genes and a mutation in this gene is found in the majority of all human tumors.[6] In healthy cells, p53 accumulates in response to cellular stress, such as extensive DNA damage, and then functions as an activator in the apoptotic pathway. Mutations in the genes responsible for encoding p53 result in cells that evade apoptosis and survive despite damage that should cause them to initiate programmed cell death.[5] This type of mutation is advantageous for cancerous cells because in order to proliferate without control in non-native environments they need to evade checkpoints that function to kill cells with these characteristics. Several other oncogenes have been discovered that are a part of the apoptotic pathway. The protein Bcl-2 is known to act as an anti-apoptosis signal and is often over expressed in cancerous cells. Some oncogenes are actually responsible for promoting apoptosis, one example is Myc which functions as both a promoter of cell proliferation and a promoter of apoptosis.[5] This dual functionality is a useful control in healthy cells because it ensures that cells need both an activating signal from Myc and an anti-apoptotic signal in order to continue proliferating. However, in the presence of consistent anti-apoptosis signals such as when bcl-2 is overexpressed, the proliferating activity of Myc continues to be active allowing the cells to continuously divide without initiating cell death.[5]

Even though apoptotic pathways are often malfunctioning in cancerous cells, the induction of apoptosis is an important aim of many cancer treatments. The complex relationship between tumor development and alterations of the cells' ability to initiate programmed cell death makes apoptosis an interesting target for cancer treatments; the goal is to trigger apoptosis more readily in the mutated cells than in the patients' healthy cells.[7] Tumors with mutations in genes such as p53 have increased risk of being resistant to these treatments because of their inactivated apoptotic pathways. On the other hand, tumors that have activated oncogenes such as Myc are often more receptive to treatment because apoptosis can be triggered more easily.[5] Chemotherapeutic drugs that induce apoptosis in tumor cells also promote apoptosis in healthy cells, which is one of the causes of cytotoxicity and other negative side effects experienced with chemotherapy.[6] Some current studies are focusing on designing chemotherapy drugs that target specific effector molecules within the apoptosis pathway, however historically many successful chemotherapy drugs have the simple aim of damaging DNA in order to promote apoptosis. It is important to note that inflicting DNA damage on cancerous cells also has the ability to promote other types of cell death such necrosis, mitotic catastrophe, autophagy, and early senescence. Historically a focus had been placed on apoptosis, however the ability to selectively induce cell death in any capacity is a promising characteristic of any potential anti-cancer agent.[8]

*1.2 Cancer treatments currently available and how they function*

For the most part cancer treatments fall into three main categories: surgery, radiation, and chemotherapy. Many cancer treatment plans involve the use of two or

more of these treatments administered either simultaneously or in succession.[9] Surgery is typically used for cancers that are isolated and have yet to metastasize. In this case the goal of surgery is to remove the entirety of the tumor and sometimes radiation or chemotherapy is administered post operatively to kill off any cancerous cells the surgery may have missed. Alternatively, surgery can be used to reduce the size of a large tumor that cannot be removed entirely before starting radiation or chemotherapy to increase the chances of success with one of these treatments.[9] Radiation therapy uses X-rays to eliminate tumors. The concept behind this treatment is that the X-rays will induce DNA damage within the exposed cells and the actively dividing mutated cancer cells will be less able to repair this damage than healthy cells, promoting an increased rate of cell death in the cancerous cells. Since this treatment relies on damaging DNA there is a small risk that a patient will develop a different cancer as a result of receiving radiation therapy.[9]

The final category of available treatment options is chemotherapy, which actually encompasses a wide range of cytotoxic drugs that work by inhibiting cellular growth or promoting cell death. One of the benefits of this type of treatment is the fact that it's systemic so it can be used for cancers that are not tumorous and those that have metastasized before they have formed masses large enough to detect.[9] Since the aim of these drugs is to disrupt cell proliferation the target of their activity is often DNA, because the cells need functional DNA in order to replicate and proceed through the cell cycle. Some of these agents work by altering the structure of DNA bases thus limiting reactivity of enzymes involved in replication, some work by creating crosslinks between

the bases so that they cannot be separated and others are successful by causing breaks on one or both strands in the double helix.[9]

*1.3 Metal complexes as chemotherapy agents*

Platinum-containing complexes such as cisplatin, carboplatin and oxaliplatin are all examples of metal complexes that have been approved for use as chemotherapy drugs.[10] The structure of each of these complexes is shown in Figure 1.

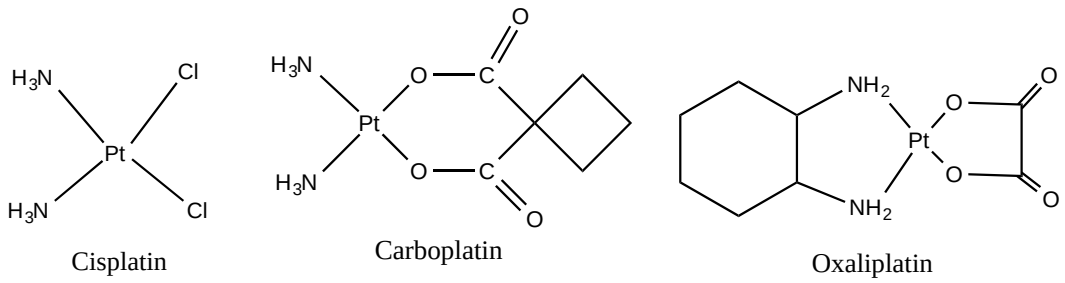


Cisplatin Carboplatin Oxaliplatin

**Figure 1.** Structures of cisplatin, carboplatin, and oxaliplatin. (Figures taken from *Clinical Status of Cisplatin, Carboplatin, and Other Platinum-Based Antitumor Drugs*[13])

Cisplatin is known to work by covalently boding to DNA and creating cross-linkages, which causes the DNA to kink and become inaccessible to DNA replication machinery.[10,11] Once cisplatin crosses the membrane and enters a cell it is surrounded by an aqueous environment with a lower chloride concentration; as a result one of the chloride groups is typically replaced with a water molecule. After water has bound to cisplatin, the complex becomes a positively charged species that is highly reactive with DNA's negatively charged backbone.[10] Cisplatin is known to preferentially bind with deoxyguanosines and create interstrand, intrastrand, and DNA-protein cross-linkages.

Interstrand cross-linkages result from one cisplatin binding to two bases on opposite strands of the double helix, whereas intrastrand cross-linkages result from binding to two bases on the same strand. These alterations of the DNA, shown in Figure 2, are thought to be the main source of cisplatin's cytotoxicity because the damage often induces apoptosis.[10,11] Radio-labeling has shown that the majority of linkages formed are intrastrand and it is generally accepted that these linkages contribute most to cisplatin's overall cytotocity.[12,13] Due to the damage interrupting DNA replication, the cytotoxicity is specific to rapidly dividing cells, such as cancerous ones. Cisplatin has been used to effectively treat testicular, ovarian, lung, head, neck, and bladder cancers.[14] Although the success of cisplatin has made great improvements in cancer treatment and survival, it is also linked to a number of negative side effects including nephrotoxicity and neurotoxicity. As a result, the search for cisplatin analogs that are less toxic to healthy cells and ultimately less damaging to the patient continues to be at the forefront of research efforts.

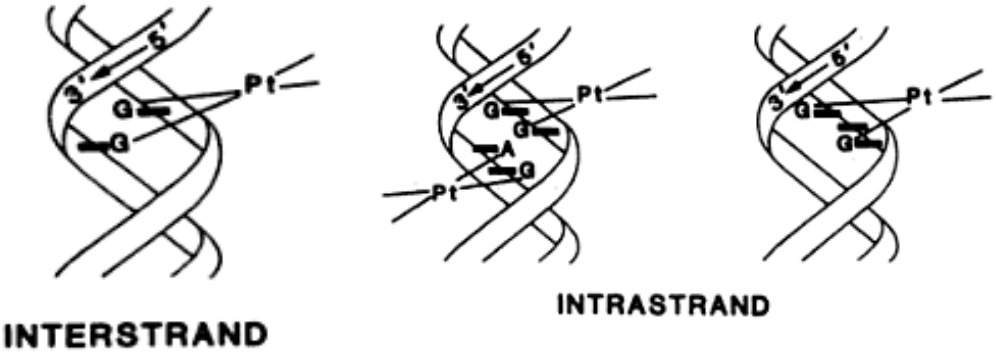


Figure 2. Structure of interstrand and intrastrand adducts on DNA caused by cisplatin. (Figures taken from: The Mechanism of Action of Cisplatin: From Adducts to Apoptosis [11])

Carboplatin was designed as a cisplatin analog. The design behind the synthesis

of this drug was replacing the labile chloride groups in cisplatin with more stable ligands in an effort to lower the overall toxicity of the compound, in order to minimize negative effects on healthy cells. As hoped, carboplatin proved less toxic than cisplatin and has similar effectiveness as an anti-cancer drug by causing similar adducts on DNA.[14]

Oxaliplatin is a cisplatin analog that not only has more stable ligands in place of chloride groups, but also has diaminocyclohexane in place of the two amine groups. Similarly to cisplatin, this anti-cancer agent is known to function by inducing three different types of crosslinks on DNA: intrastrand, interstrand, and DNA-protein. As with the other complexes these crosslinks serve to arrest the cell cycle and eventually promote apoptosis. Although the main mode of inflicting DNA damage seems to be the same, the structural differences have allowed oxaliplatin to be useful in the treatment of digestive system cancers, which are untreatable with cisplatin and carboplatin.[15]

Although these three platinum containing compounds have been successful in treating certain types of tumors, their usage faces certain restrictions. These obstacles include cells building resistance to platinum-based anti-cancer drugs, the toxicity of the metal having negative impacts on the rest of the body, and an insufficient amount of uptake by the cell. Some studies have used the properties of copper in order to aid the transport of platinum-based complexes, because specific channels exist to allow its transport into the cell.[16]

*1.4 Copper based compounds as potential chemotherapeutic agents*

Copper is naturally occurring in the body and its role in redox chemistry makes it an essential element needed for many basic biochemical reactions. Ideally the bioavailability of copper will result in lower toxicity levels of copper containing anti-cancer complexes compared to other non-essential transition metals such as platinum.[17] Additionally, it has been found that copper concentrations are elevated in tumors and its presence is thought to be essential for angiogenesis.[18] Overall, copper complexes show great potential as anti-cancer agents because the metal involved may be selectively shuttled to cancerous masses within the body.

The reactivity of copper complexes is assessed by DNA cleavage, protein binding, and DNA binding. Previously, in the Tyler research group utilized ligand frames containing substituted thiazole groups, specifically where R= 8-hydroxyquinoline, 2-pyridine, and 2-quinoline. The synthetic scheme for these ligands is shown in Figure 3.

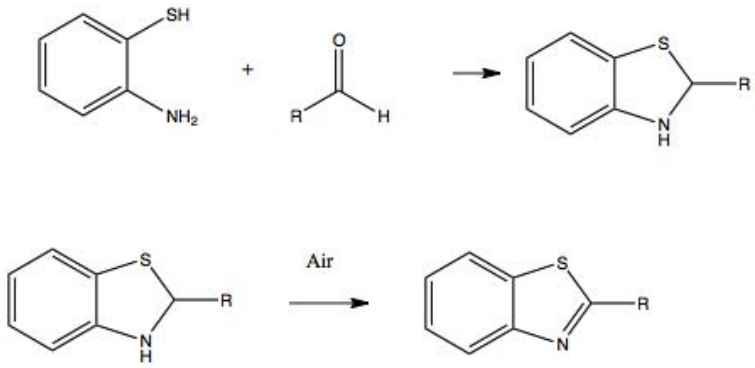


**Figure 3.** Reaction for thiazole ligand compounds, where R represents the groups being altered.

Several corresponding Cu(II) complexes with these ligands have been isolated and characterized. The complexes shown in Figure 4 were tested for biological activity by lab members Han Lin and David Foreman.[19,20] These complexes were assessed for biological activity using the aforementioned criteria DNA binding, protein binding, and DNA cleavage.

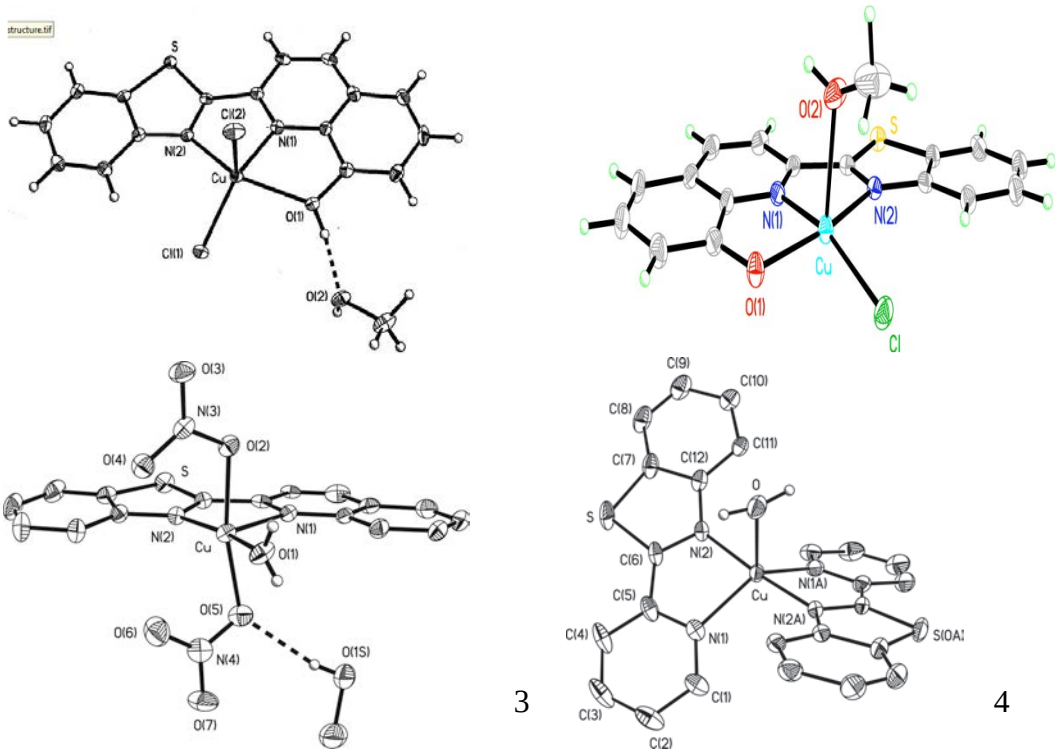


**Figure 4**. Crystal structures of $Cu(8OHQ(oBt))Cl_2$ (**1**) $Cu(8OQ(oBt))Cl\ (MeOH)$ (**2**) $Cu(Q(oBt))(H_2O)(NO_3)_2$ (**3**) and $[Cu(Py(oBt))_2H_2O]^{2+}(BF_4)_2$ (**4**) [19.20]

Studies of the compounds shown in Figure 4 demonstrated that the structural differences between them influenced their efficiency for DNA cleavage and the strength of DNA binding. DNA cleavage studies indicated that compound **2** had the greatest DNA cleavage efficiency while compound **4** had the least efficiency. DNA binding studies using EtBr indicated that compound **1** intercalates DNA with the greatest strength and

compound **4** intercalates with the least strength. Protein binding studies did not provide comparative results because binding constants were not determined.[19]

This project is an extension of the aforementioned work. I have synthesized new thiazole based ligands and the corresponding copper complexes. These complexes have been tested for biological activity in the same manner as those previously studied and reactivity and binding strength comparisons have been made between all the complexes tested up to this point.

## 2. Experimental

### *2.1 Material*

All starting materials were purchased from Sigma Aldrich and were used in their original condition without further purification. Anhydrous solvents were also purchased from Sigma Aldrich and left untreated.

### *2.2 Instruments*

$H^1$ NMR spectra were collected using a 400 MHz Brüker Avance NMR spectrometer. Infrared spectra were collected using a Nicolet Avatar 330 FT-IR with smart orbit solid-state attachment. Absorbance spectra were obtained using an Agilent 8453 spectrophotometer. Fluorescence spectra were collected using an 810 Photomultiplier Detection System spectrophotometer. A Bio Rad PowerPac 300 was used for DNA separation via agarose gel electrophoresis. Gel images were recording using a

Syngene G:Box and analysis of band density was performed using the Syngene:GeneTools program.

### *2.3 Preparation of Ligands*

#### *2.3.1 PyOMe(oBt)*

The ligand, PyOMe(oBt), was synthesized in the following way: 346 µL (2.88 mmol) of 6-methoxy-2-pyridine carboxaldehyde and 308 µL (2.88 mmol) of 2-aminothiophenol were added to ~20 mL of ethanol (EtOH). The reaction was refluxed for 1 h. After refluxing, the solution was left to heat open to air for an additional hour, as a result the volume was reduced to ~5 mL via evaporation and a white precipitate formed. The product was collected via vacuum filtration, washed with EtOH, and then dried under vacuum for 1 h. Yield: 755 mg (47%). $^{1}$H NMR ($CDCl_3$, 400 MHz, 25º C, δ from TMS): 8.08 (d, 1H, *J* = 8.16 Hz), 7.95 (m, 2H), 7.728 (m, 1H), 7.50 (m, 1H), 7.40 (m, 1H), 6.86 (d, 1H, *J* = 8.24 Hz), 4.07 (s, 3H). Selected IR bands: ($cm^{-1}$) 1574 ($\nu_{N=C}$), 1421 (s), 724 (s), 801 (m).

#### *2.3.2 PyOMe(en)*

The ligand, *PyOMe(en)*, was synthesized in the following way: 720 µL (5.98 mmol) of 6-methoxy-2-pyridine carboxaldehyde and 200 µL (2.99 mmol) of ethylene diamine (en) were added to ~30 mL of EtOH. The reaction was refluxed for 1 h resulting in a color change to bright yellow. The solution volume was then reduced to ~10 mL via rotoevaporation resulting in the formation of a white solid. The product was collected via vacuum filtration, rinsed with hexanes, and then dried under vacuum for 1 h. Yield: 311.4

mg (49%). $^{1}$H NMR ($CDCl_3$, 400 MHz, 25° C, δ from TMS): 8.30 (s, 1H), 7.58 (m, 2H), 6.76 (d, 1H, *J* = 7.72 Hz), 4.02 (s, 2H), 3.95 (s, 3H). Selected IR bands: ($cm^{-1}$) 1587 ($\nu_{N=C}$), 1019(m), 730 (s).

*2.4 Synthesis of Complexes*

*2.4.1 Cu(PyOMe(oBt))$Cl_2$ (**1**)*

First, the ligand PyOMe(oBt) (260.9 mg, 1.10 mmol) was dissolved in ~10 mL MeOH. Separately, copper chloride (185.8 mg, 1.10 mmol) was dissolved in ~5 mL MeOH. Next, the metal solution was added dropwise to the ligand solution. The solution turned a deep brown color upon addition of the metal salt. The solution was stirred for 24 h and then gravity filtered. Upon slow diffusion of diethyl ether ($Et_2O$) into this brown solution resulted in the formation of, orange-brown, block like crystals. Yield: 166 mg (17.1%). Selected IR bands: ($cm^{-1}$) 1573 ($\nu_{N=C}$), 1429 (s), 732 (s), 806 (m). Electronic absorption spectrum in MeOH: $\lambda_{max}$ (nm) (ε, $M^{-1}$ $cm^{-1}$) 322 (40213).

*2.4.2 [Cu(PyOMe(oBt)$_2$($NO_3$)]$NO_3$ (**2**)*

Ligand, PyOMe(oBt) (192.7 mg, 0.82 mmol) and copper nitrate (95.2 mg, 0.41mmol) were separately dissolved in ~10 mL of methanol (MeOH). Next, the metal was added dropwise to ligand. Upon addition of the metal the solution turned brown-yellow and a lime green solid formed almost immediately. The solution was allowed to stir for 6 h and then gravity filtrated. Upon slow diffusion of acetonitrile (ACN), the brown solution turned a bright green color similar to the initial solid collected. The solution was then left to slowly evaporate. After several days large green block like

crystals had formed. Yield: 62.8 mg (27.5%). Selected IR bands: ($cm^{-1}$) 1427 (s), 728 (s), 808 (m). Electronic absorption spectrum in MeOH: $\lambda_{max}$ (nm) ($\varepsilon$, $M^{-1}$ $cm^{-1}$) 322 (34194).

### *2.4.3 $[Cu_2(PyOMe(en))(PyOMe(enH_2)_2](NO_3)_4$ (**3**)*

First, the ligand PyOMe(en) (217.8 mg, 0.73mmol) was dissolved in ~10 mL anhydrous MeOH then copper nitrate (169.8 mg, 0.73mmol) was separately dissolved in ~10 mL anhydrous MeOH. Next, the metal solution was added dropwise to the ligand solution. The colorless solution turned a deep aqua color upon addition of the metal solution. The solution was stirred for 24 h and then gravity filtered. Upon slow diffusion of $Et_2O$ into the solution, deep blue crystals formed. Yield: 45.5 mg (19.1%). Selected IR bands: ($cm^{-1}$) 1592 ($\nu_{N=C}$), 999(m), 732 (s).

## *2.5 Solution Preparations*

### *2.5.1 TAE Buffer (1X)*

50X TAE Buffer was prepared at outlined in *Fox Research Lab Protocols*.[21] 20 mL of the 50X buffer was then diluted to a final volume of 2 L with deionized water.

### *2.5.2 Tris-HCl Buffer (5 mM Tris, pH 7.2) 50 mM NaCl*

First, Tris (151.4 mg) was dissolved in ~ 200 mL of deionized water and then NaCl (730 mg) was also added into the solution. The desired pH was reached by titrating with 0.1M HCl and/or 0.1M KOH while monitoring the solution using a pH electrode.

Once a pH reading of 7.2 was reached the solution was diluted to a final volume of 250 mL with deionized water in a graduated cylinder.

*2.5.3 Stock Complex Solutions (1000 μM)*

Complex **1** (7.5 mg) and **2** (7.1 mg) were weighed out using an analytical balance and then separately diluted to a final volume of 10 mL with dimethylformamide (DMF) in a volumetric flask. The solution was shaken until complex was completely dissolved and then stored at room temperature and used within 24 h of preparation.

*2.5.4 Ascorbic Acid Stock Solution (2000 μM and 1000 μM)*

The stock solution was prepared by first obtaining 3.52 mg and 1.76 mg of ascorbic acid respectively diluting to a final volume of 10 mL with 5 mM Tris, 50 mM NaCl pH 7.2 Buffer (prepared as outlined above) in a volumetric flask. Solid was dissolved via shaking and then solutions were stored at 12°C for future use.

*2.5.5 Plasmid DNA Preparation*

The plasmid DNA preparation was performed by first transforming E.coli cells via electroporation using the procedure outlined in *Fox Research Lab Protocols (1-9).*[21] Once the cells were transformed the procedure for plasmid mini-prep was followed (*Fox Research Lab Protocols (1-12)).*[21] Once a purified sample of plasmid DNA was obtained the concentration was determined using the nanodrop by following the procedure outlined in *Fox Research Lab Protocols (2-1).*[21]

### *2.5.6 Calf Thymus DNA (CT-DNA) Stock Solution*

CT-DNA stock solution was prepared using the procedures outlined in Foreman *et al.*[20]

### *2.5.7 Bovine Serum Albumin (BSA) Stock Solution (50 μM)*

BSA stock solution was prepared using the procedures outlined in Foreman *et al.*[20]

## *2.6 Biological Studies*

### *2.6.1 DNA Cleavage and Mechanistic Studies*

DNA cleavage studies were performed by preparing ten different solutions of varying complex concentration that were composed of 5 mM Tris, 50 mM NaCl, pH 7.2 buffer, ascorbic acid at a concentration twice that of the given complex concentration, and plasmid DNA of a constant concentration of 0.01 μg/μL. Buffer was added to ensure each sample had a final volume of 30 μL and were prepared in accordance with the amounts shown in Table 1. Plasmid DNA was always added last and the final solution was mixed by pipetting up and down.

**Table 1.** Sample preparation for DNA cleavage studies using 1000 μM stock complex solution and 1000 μM stock ascorbic acid solution.

| Lane # | Complex Concentration (μM) | Compound volume (μL) | DNA volume (μL) | [AH2] (μM) | AH2 volume (μL) | Buffer volume (μL) |
|---|---|---|---|---|---|---|
| 1 | 0 | 0 | 1 | 0 | 0 | 29 |
| 2 | 100 | 3 | 1 | 200 | 6 | 20 |
| 3 | 125 | 3.75 | 1 | 250 | 7.5 | 17.75 |
| 4 | 150 | 4.5 | 1 | 300 | 9 | 15.5 |
| 5 | 175 | 5.25 | 1 | 350 | 10.5 | 13.25 |
| 6 | 200 | 6 | 1 | 400 | 12 | 11 |
| 7 | 225 | 6.75 | 1 | 450 | 13.5 | 8.75 |
| 8 | 250 | 7.5 | 1 | 500 | 15 | 6.5 |
| 9 | 275 | 8.25 | 1 | 550 | 16.5 | 4.25 |
| 10 | 300 | 9 | 1 | 600 | 18 | 2 |

The DNA cleavage mechanistic studies were performed in a similar experimental set up was used. Ten solutions of varying complex concentration with the same composition shown in Table 1, except these experiments included the addition of either L-histidine or DMSO. The volumes of each solution present in each of these samples are outlined in Table 2 and Table 3.

**Table 2.** Sample preparation for L-histidine mechanistic studies using 1000 μM stock complex solution and 2000 μM stock ascorbic acid solution and 50 mM stock of L-histidine.

| Lane # | Compound (μM) | Compound (μL) | DNA (μg/μL) | DNA (μL) | [AH2] (μM) | AH2 (μL) | L-Histidine (μM) | L-Histidine (μL) | Buffer (μL) |
|---|---|---|---|---|---|---|---|---|---|
| 1 | 0 | 0 | 0.01 | 1 | 0 | 0 | 2000 | 1.2 | 27.8 |
| 2 | 100 | 3 | 0.01 | 1 | 200 | 3 | 2000 | 1.2 | 21.8 |
| 3 | 125 | 3.75 | 0.01 | 1 | 250 | 3.75 | 2000 | 1.2 | 20.3 |
| 4 | 150 | 4.5 | 0.01 | 1 | 300 | 4.5 | 2000 | 1.2 | 18.8 |
| 5 | 175 | 5.25 | 0.01 | 1 | 350 | 5.25 | 2000 | 1.2 | 17.3 |
| 6 | 200 | 6 | 0.01 | 1 | 400 | 6 | 2000 | 1.2 | 15.8 |
| 7 | 225 | 6.75 | 0.01 | 1 | 450 | 6.75 | 2000 | 1.2 | 14.3 |
| 8 | 250 | 7.5 | 0.01 | 1 | 500 | 7.5 | 2000 | 1.2 | 12.8 |
| 9 | 275 | 8.25 | 0.01 | 1 | 550 | 8.25 | 2000 | 1.2 | 11.3 |
| 10 | 300 | 9 | 0.01 | 1 | 600 | 9 | 2000 | 1.2 | 9.8 |

**Table 3**. Sample preparation for DMSO mechanistic studies using 1000 μM stock complex solution and 2000 μM stock ascorbic acid solution and pure DMSO.

| Lane # | Compound (μM) | Compound (μL) | DNA (μg/μL) | DNA volume (μL) | [AH2] (μM) | AH2 (μL) | DMSO (μL) | Buffer (μL) |
|---|---|---|---|---|---|---|---|---|
| 1 | 0 | 0 | 0.01 | 1 | 0 | 0 | 3 | 26 |
| 2 | 100 | 3 | 0.01 | 1 | 200 | 3 | 3 | 20 |
| 3 | 125 | 3.75 | 0.01 | 1 | 250 | 3.75 | 3 | 18.5 |
| 4 | 150 | 4.5 | 0.01 | 1 | 300 | 4.5 | 3 | 17 |
| 5 | 175 | 5.25 | 0.01 | 1 | 350 | 5.25 | 3 | 15.5 |
| 6 | 200 | 6 | 0.01 | 1 | 400 | 6 | 3 | 14 |
| 7 | 225 | 6.75 | 0.01 | 1 | 450 | 6.75 | 3 | 12.5 |
| 8 | 250 | 7.5 | 0.01 | 1 | 500 | 7.5 | 3 | 11 |
| 9 | 275 | 8.25 | 0.01 | 1 | 550 | 8.25 | 3 | 9.5 |
| 10 | 300 | 9 | 0.01 | 1 | 600 | 9 | 3 | 8 |

Once the solutions were prepared the procedure for the DNA cleavage studies and the mechanistic studies was identical. The solutions were left to incubate at 37°C for 2 h. After incubation the samples were centrifuged at maximum speed in the microfuge for 5 min and then 10 μL from each sample was transferred to a separate tube. Next, 2 μL of 6X loading dye was mixed into the 10 μL samples and then the total volume of 12 μL was loaded into a 1% agarose gel in 1X TAE running buffer. The gel was prepared using the procedure outlined in *Fox Research Lab Protocols (3-1).*[21] The gel was run at 80 V for 1 h 15 min and then stained in 0.5 μg/mL EtBr for 30 min. After staining, the gel was de-stained in deionized water for 10 min.

### *2.6.2 DNA Binding Ethidium Bromide (EtBr) Fluorescence Studies*

DNA Binding studies were performed using the procedures outlined in Foreman *et al* and Lin *et al.*[19,20]

### *2.6.3 Bovine Serum Albumin (BSA) Binding Fluorescence Studies*

*BSA* binding studies were performed using the procedures outlined in Foreman *et al* and Lin *et al.*[19,20]

## 3. Results and Discussion

### *3.1 Synthesis and Characterization of Ligands*

The ligands PyOMe(oBt) and PyOMe(en) were synthesized by reacting 6-methoxy-2-pyridine carboxaldehyde with 2-aminothiophenol and ethylene diamine,

respectively. The reactions were carried out in methanol and the structures of these ligands were confirmed via IR and $^{1}$H-NMR spectroscopies. The PyOMe(oBt) ligand was formed via the condensation reaction shown in Scheme 1. The initial product formed was typically the thiazoline intermediate shown (Scheme 1, line 2, left), however upon oxidation in air only the final thiazole product was obtained. The two different products can be distinguished using $^{1}$H-NMR spectroscopy based upon the disappearance of the peaks associated with –NH and –CH shifts.[22] Appendix 1 depicts the $^{1}$H-NMR spectrum of the final thiazole product, PyOMe(oBt), which lacks both of these characteristic thiazoline peaks and contains peaks and integration expected for the thiazole product. The PyOMe(en) ligand was formed via the reaction shown in Scheme 2, which also results in the formation of $H_2O$ as a byproduct. The condensation reaction could possibly lead to both the mono- and disubstituted amine. $^{1}$H-NMR spectroscopy was used to confirm that the product isolated was the disubstituted ligand containing two imine groups based on the absence of a peak corresponding to $NH_2$. The $^{1}$H-NMR spectrum of the final product is shown in Appendix 2.

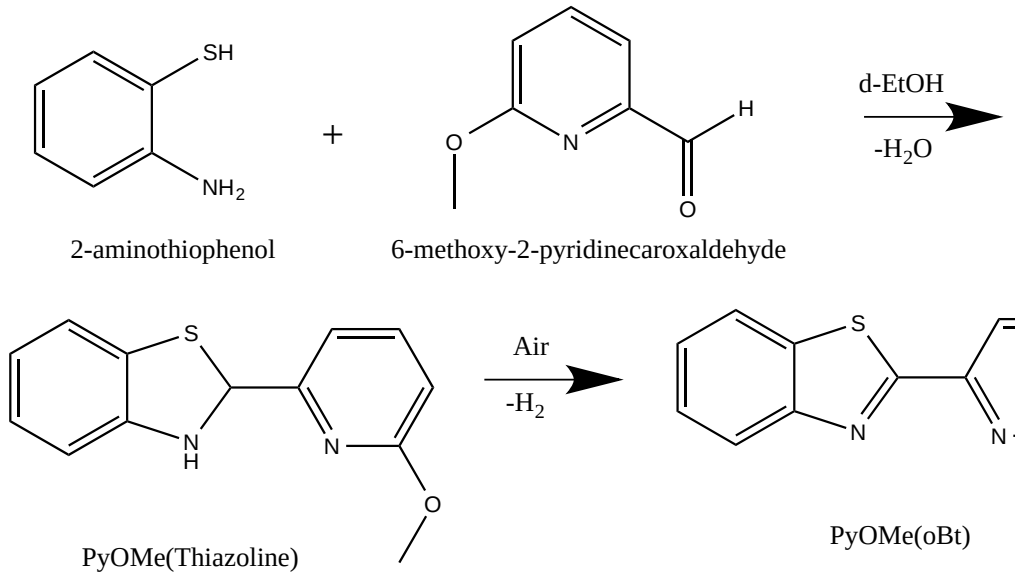


**Scheme 1.** Reaction scheme for synthesis of PyOMe(oBt) ligand. Top: condensation of 2-aminothiophenol with 6-methoxy-2-pyridinecarboxaldehyde to form the corresponding thiazoline. Bottom: air oxidation of the thiazoline to afford the thiazole containing ligand.

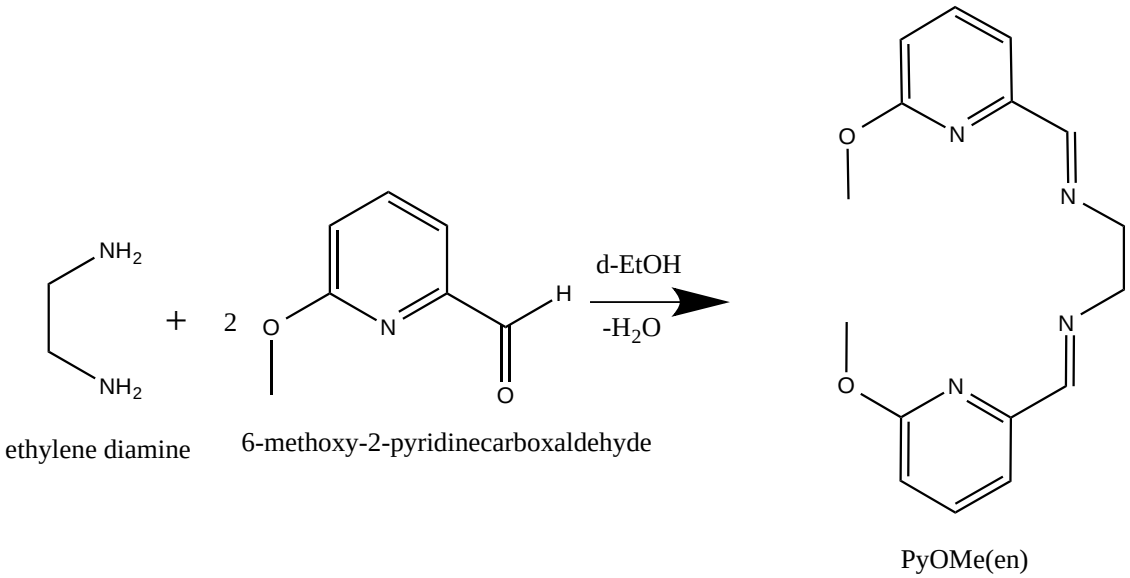


**Scheme 2.** Reaction scheme for synthesis of PyOMe(en) ligand. Condensation of ethylene diamine with 6-methoxy-2-pyridinecarboxaldehyde.

*3.2 Synthesis and Characterization of Cu(II) Complexes*

The corresponding copper(II) complexes were obtained for both ligands. Interestingly, two complexes were isolated for the PyOMe(oBt) ligand as a result of reacting it with both $CuCl_2$ and $Cu(NO_3)_2$, respectively. A single complex was isolated for the PyOMe(en) ligand. This complex was a product of the ligand's reaction with $Cu(NO_3)_2$. Structures of these complexes were determined via X-ray crystallography. Thermal ellipsoid plots showing the crystal structures of these complexes are shown in Figure 5.

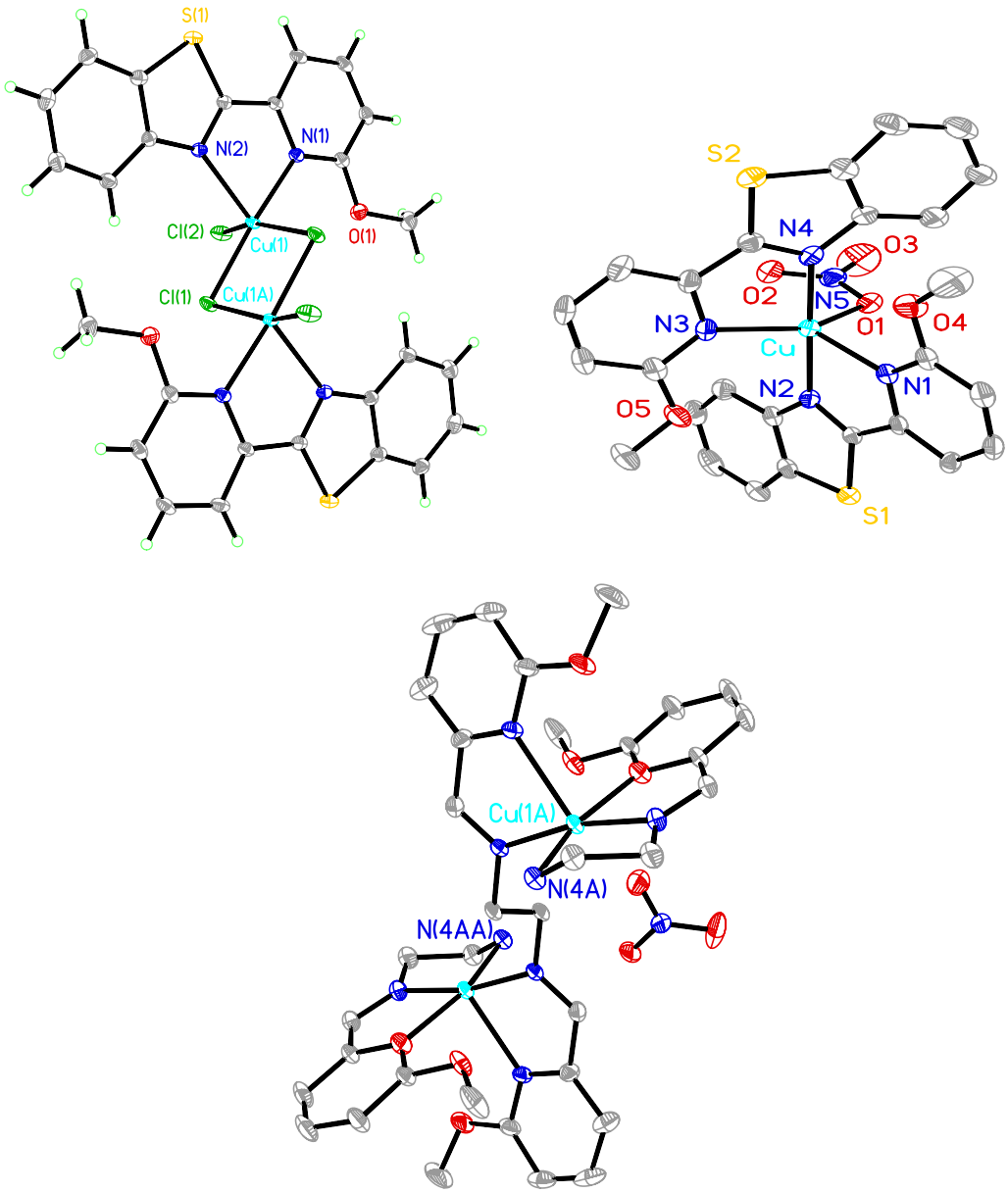


**Figure 5**. Thermal ellipsoid plots (50% probability level) of complexes **1** (top left), **2** (top right), and **3** (bottom). For complexes **2** and **3,** H atoms and $NO_3^-$ counter ions have been omitted for clarity.

Synthesis of complex **1** resulted in the formation of orange-brown crystals with block like morphology. Ligation of the ligand was confirmed by analysis of the IR spectrum of the complex compared to the IR spectrum of the free ligand (Appendix 3). Upon coordination, the spectrum revealed several resonances that shifted to lower energy

indicative of coordination (Appendix 4). X-ray analysis showed that complex **1** is a dimer with two copper centers ligated to one ligand (N,N). The coordination sphere around each copper is completed by two chloride ions, one terminal and one bridging. The bond length between Cu-$N_{Py}$ is 2.020 Å, whereas the bond length between Cu-$N_{thiazole}$ is 2.271 Å. The bond angle between these three atoms is 77.7°. The bond angle between $N_{Py}$-Cu-Cl was 91.1° and the angle between $N_{thiazole}$-Cu-Cl was 104.4° giving rise to distorted trigonal bipyrimidal geometry around each metal center.

Synthesis of complex **2** yielded large green block like crystals. The IR spectrum of these crystals is shown in Appendix 5. Upon coordination of the ligand, several IR resonances shift to lower energy, indicative of coordination. The ellipsoid plot obtained via X-ray analysis showed complex **2** is a monomer with two ligands bound to each Cu(II) center and one O-bound nitrate with an overall +1 charge. The $N_4O$ coordination sphere around the metal center gives rise to a distorted trigonal bipyriamidal geometry.

Synthesis of complex **3** yielded large deep blue sea urchin like crystals. Appendix 6 shows an IR spectrum of the starting ligand and Appendix 7 shows an IR spectrum of complex **3** crystals for comparison. Similar to the complexes previously mentioned, the IR spectrum of complex **3** revealed several resonances that shifted to lower energy upon coordination to the metal center. X-ray analysis yielded very interesting results because the structure of complex **3** was shown to contain two metal centers. Each copper center was ligated to one partially hydrolyzed ligand (PyOMe($enH_2$)) ligand and one unhydrolyzed ligand (PyOMe(en)) that bridged between the two metals. The geometry of

the $N_5$ coordination sphere around each metal center is best described as distorted square pyriamidal. The bond lengths between Cu-$N_{Py}$ were 2.023 and 1.962 Å with an angle of 82.5°. The bond lengths between Cu-$N_{en}$ were 2.017, 2.097, and 2.246 Å with angles of 169.1° and 77.3°. The bond angle between $N_{en}$-Cu-$N_{PyOMe}$ was 102.0°.

The observed structural differences between complexes **1** and **2** demonstrate the impact that the starting metal has on the overall structure of the complex. However, for complex **3** there were inconsistencies between the molecular weight indicated by the X-ray crystal structure and the elemental analysis data. This made it unclear whether the complex was undergoing the same extent of hydrolysis every time the reaction was carried out. Experimentation with this complex is still ongoing, however, until the molecular weight and crystal structure data match the elemental analysis for the bulk, complex **3** cannot be tested for biological activity.

*3.2 DNA Cleavage Studies*

DNA is a common target of chemotherapy drugs because of its key role in cellular proliferation. Cells require DNA that is both intact and accessible to replication machinery in order to divide. Cancer cells are particularly impacted by reagents that target DNA because of their characteristic rapid proliferation rates.[9] While some complexes' mode of action involves permanent binding to the DNA, copper complexes are known for their ability to cleave DNA. The ability of a compound to induce DNA cleavage is also known as nuclease activity. One measure that was used to assess these complexes' biological activity and potential as a chemotherapeutic agent was nuclease

activity. In particular, the biological assays were used to analyze how the differing structures impact the overall biological activity.

In order to test the complexes' ability to cleave DNA the complexes were incubated with plasmid DNA in the presence of ascorbic acid. Complex concentrations ranged from 100 to 300 μM and were increased in 25 μM increments. A blank was also run without any complex present. Once the samples were incubated with the complex agarose gel-electrophoresis was used to separate the DNA based on size. Plasmid DNA can exist in several different conformations: super-coiled (SC), single-nicked (SN), and double-nicked (DN). Each of these conformations travels through the gel matrix at different rates and can therefore be distinguished from each other. This is important for these studies because each form of the DNA represents a different extent of cleavage; SC-DNA represents DNA that has not been cleaved by the complex, SN-DNA represents DNA that has been cut by the complex once, and DN-DNA represents DNA that has been cut by the complex twice. The cleavage studies, as outlined above, were carried out using complexes **1** and **2**. Figure 6 shows representative gels from these cleavage studies.

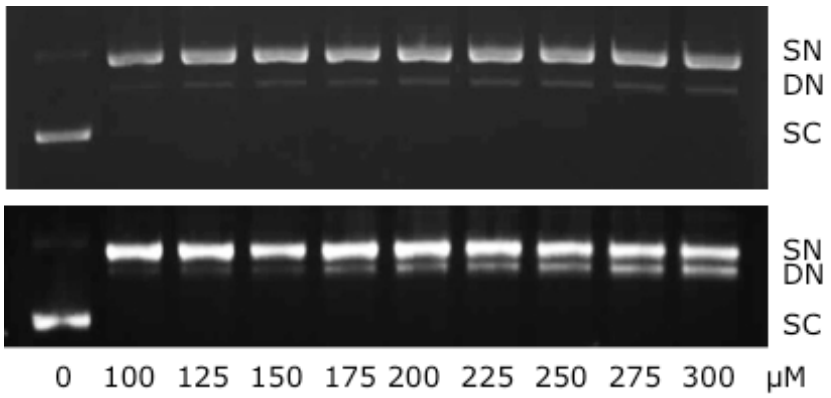


**Figure 6**. Pictures of gels from DNA cleavage studies Complex **1** (top) complex **2** (bottom). Reactions carried out at the concentrations of complex indicated below each gel in the presence of twice the concentration of ascorbic acid. Samples were incubated for 2 h at 37°C.

The gels showed that SN and DN-DNA were present in lanes that corresponded to samples incubated with complex. This indicated that the complexes are able to cleave DNA. Next, concentration dependent cleavage was determined. Band density analysis was used to determine the relative percentages of DNA in each lane on the gel. Since each lane corresponded to a given concentration of complex, complex concentration was correlated with percentages of DNA in each form. Bar graphs that show the percentages of DNA in each form at every concentration of complex **1** and **2** tested are depicted in Figure 7.

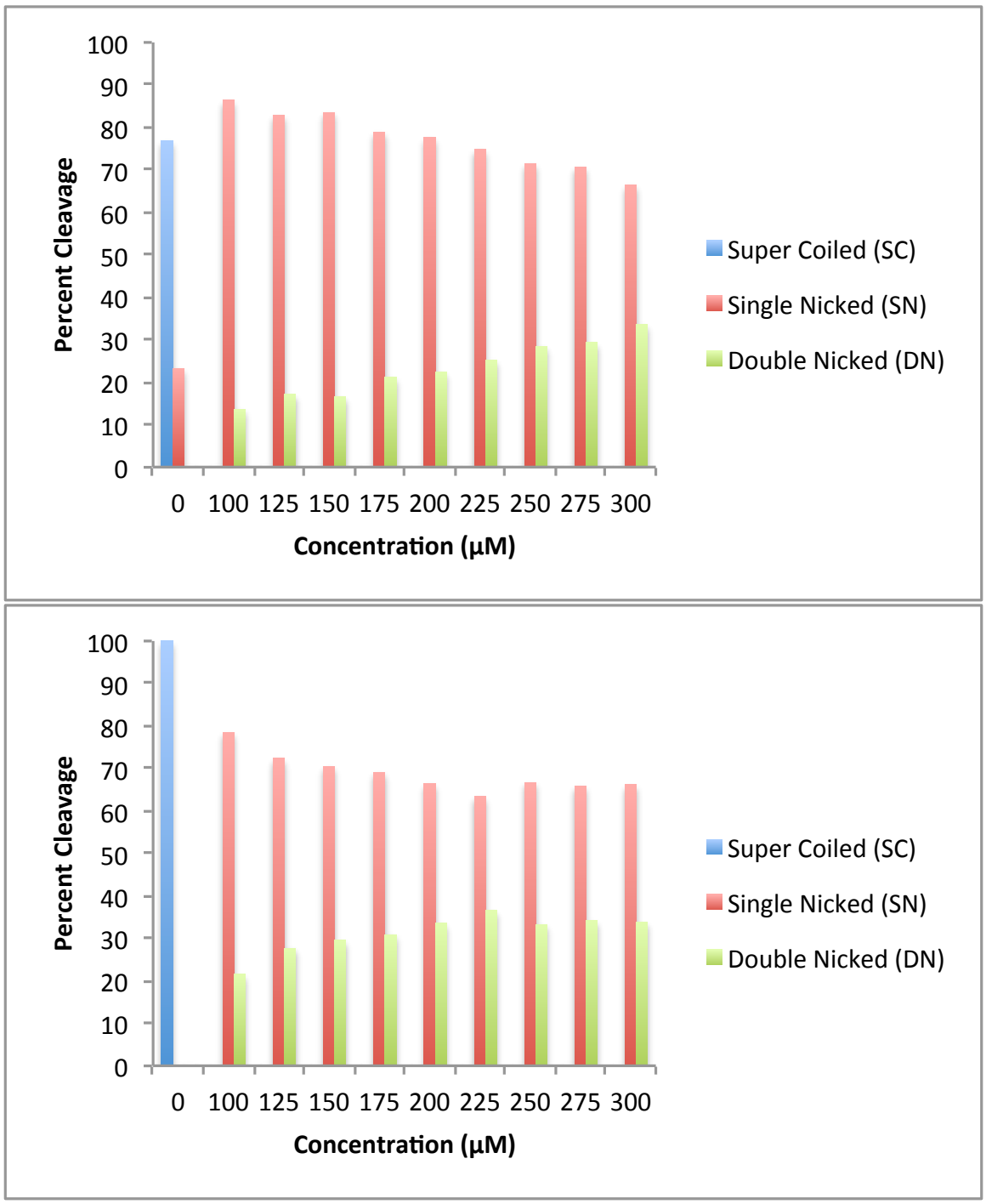


**Figure 7.** Relative percentages of DNA forms for concentration dependent cleavage studies. Complex **1** (top) complex **2** (bottom).

The percentages of DNA in the SN and DN forms are indicative of the percentage of DNA that was cleaved by the complex. The graphs show that even at the lowest concentrations of complex **1** and **2** all of the DNA has at least been converted into the SN form. This indicates that the complex cleaved all of the DNA at least once. The percentage of DNA in the DN form is equivalent to the percentage of DNA that was cleaved by the complex twice. The graph also shows that as the concentration of complex increased the percentage of DN-DNA formed also increased. This trend indicates that both complex **1** and **2** cleave DNA in a concentration-dependent manner, because the amount of cleavage is directly related to the concentration of complex. Comparison of the two graphs shows that more DN-DNA was formed in the presence of complex **2** than in the presence of complex **1** at the same concentration. This indicates that complex **2** acts as more efficient nuclease than complex **1**. When comparing the structures of these two complexes the differences in reactivity can potentially be attributed to the positive charge on complex **2**. The DNA backbone is negatively charged so the electrostatic interaction between the DNA and the positively charged complex (**2**) may be stronger than the interaction between DNA and neutral compound (**1**).

*3.3 DNA Cleavage Mechanistic Studies*

Since it was determined that the complexes were able to cleave DNA, it was of interest to determine the mechanism of this cleavage. Copper complexes are known to cleave DNA via either a hydrolytic or oxidative mechanism.[23,24] The oxidative mechanism requires the production of radical oxygen species (ROS).[25] Common ROS that have been implicated in this type of cleavage include singlet oxygen ($^1O_2$), hydroxyl

radical (•OH), and super oxide.[25,26] The hydrolytic mechanism requires water to induce nucleophilic attack of the DNA phosphate backbone.[24] Initial cleavage studies showed that in the presence of water but the absence of a reductant (ascorbic acid) needed to induce a Cu(II)/Cu(I) redox couple that generates ROS[2], the complexes did not exhibit cleavage. This indicates that a hydrolytic mechanism is not invoked in the DNA cleavage exhibited by complexes **1** and **2**. In order to ascertain if an oxidative mechanism was followed, DNA cleavage reactions were carried out with the addition of known radical oxygen scavengers. These scavengers remove all the ROS of a particular type from solution. The underlying motivation for conducting these studies is that if the removal of a particular ROS impacts reactivity, then that implicates that ROS in the mechanism as well as confirms that an oxidative mechanism is followed.

Studies were carried out using L-histidine, which is a known singlet oxygen ($^1O_2$) scavenger.[27] These reaction were carried out by incubating the DNA with varying concentration of complex in the presence of a constant concentration of L-histidine (Fig. 8). The gels show that single nicked DNA was formed but DN-DNA was not. This contrasts with the results of the initial cleavage studies carried out in the absence of scavenger, which did show the production of DN-DNA. Figure 9 shows bar graph representations of the relative amounts of SC and SN-DNA at each concentration of complex **1** and **2**. The graphs show quantitatively that DN-DNA was not formed and the percentage of SN-DNA was decreased when compared with initial cleavage studies. The observed decrease in DNA cleavage in the presence of L-histidine indicates that $^1O_2$ plays a mechanistic role in the cleavage of DNA by complex **1** and **2**. The fact that SN-DNA

was still formed but in lower quantities indicated that the $^1O_2$ species may play a more minor role in the conversion of SC-DNA to SN-DNA. The complete inhibition of the formation of DN-DNA indicated that $^1O_2$ plays a major role in the conversion of SN-DNA to DN-DNA.

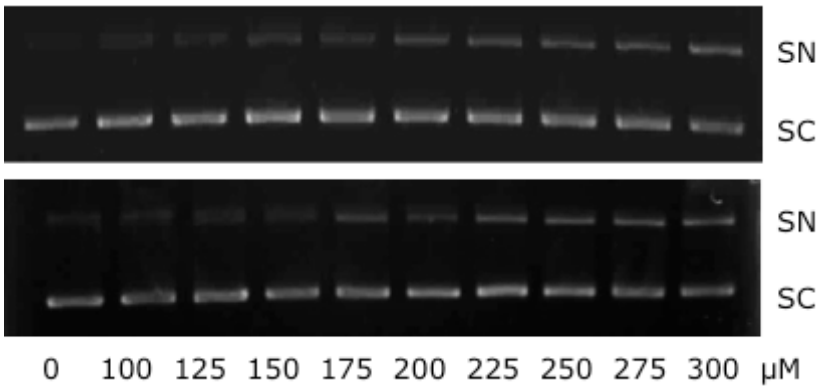


**Figure 8.** Pictures of gels from DNA cleavage mechanistic studies using L-histidine. Complex **1** (top) complex **2** (bottom). Reactions carried out at the concentrations of complex indicated in the presence of twice the concentration of ascorbic acid and a constant L-histidine concentration of 2 mM. Samples were incubated for 2 h at 37°C.

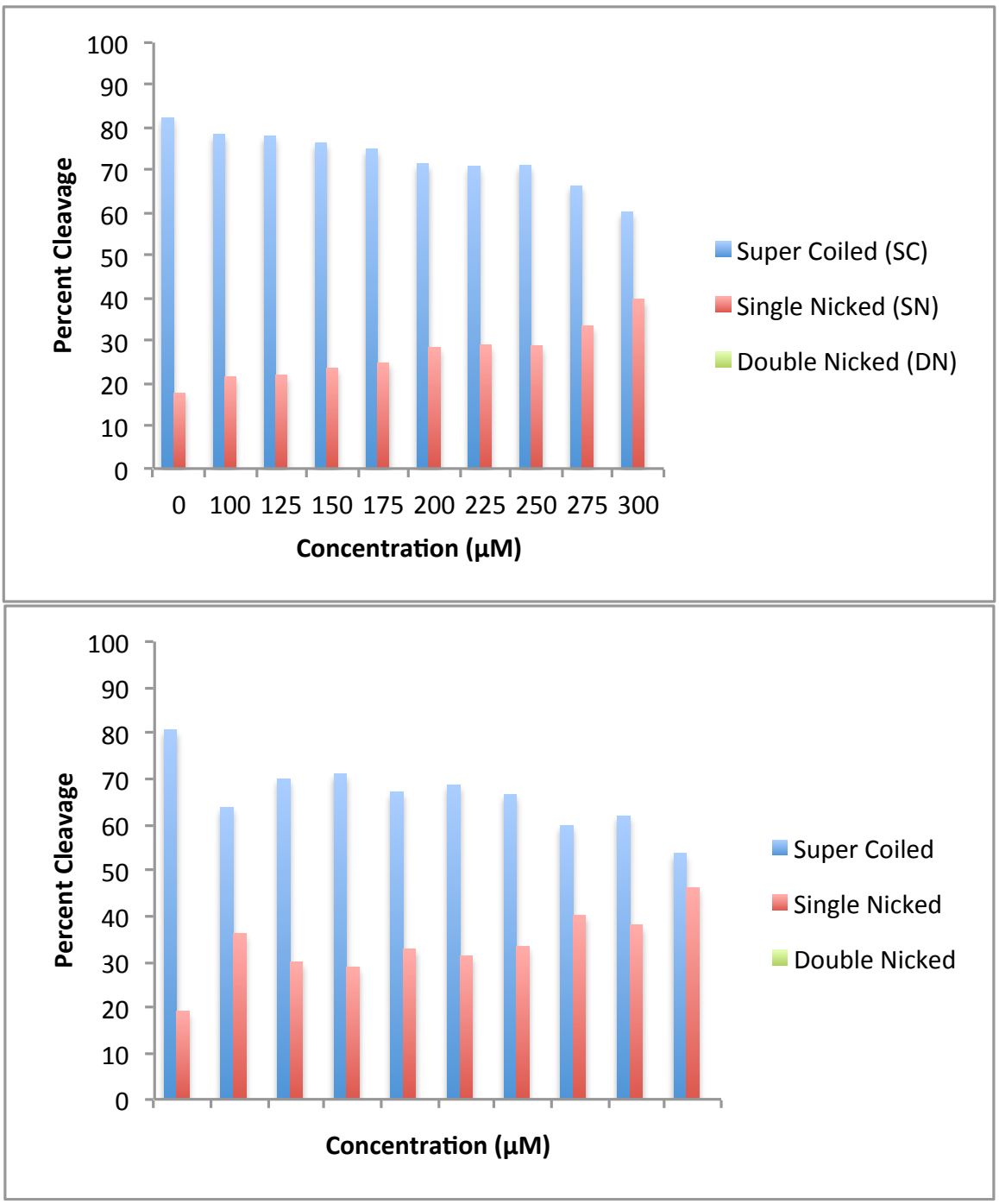


**Figure 9.** Relative percentages of DNA forms for L-histidine mechanistic studies. Complex **1** (top) complex **2** (bottom) (note: this plot is an average of two runs).

Additional mechanistic studies were conducted using DMSO, which is a known hydroxyl radical scavenger.[26] Representative gels of these studies are shown in Figure 10. These gels look very similar to the gels produced from the cleavage studies without any inhibitor, in that SN and DN-DNA forms are seen in every lane that corresponds to complex. The graphical representations, shown in Figure 11, indicated that there was no observable reactivity difference when DMSO was added into the reaction mixture. This indicates that •OH species do not play a role in the DNA cleavage mechanism for either complex **1** or **2**.

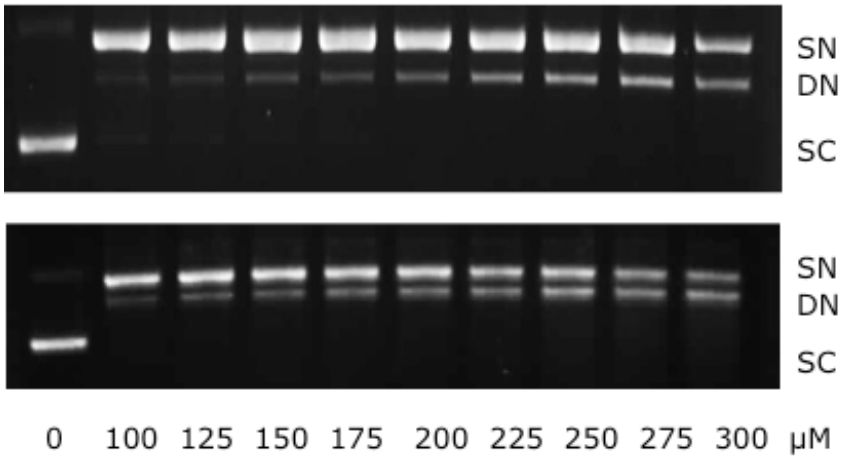


**Figure 10.** Pictures of gels from DNA cleavage mechanistic studies using DMSO. Complex **1** (top) complex **2** (bottom). Reactions carried out at the concentrations of complex indicated in the presence of twice the concentration of ascorbic acid and a constant DMSO concentration of 10% by volume. Samples were incubated for 2 h at 37°C.

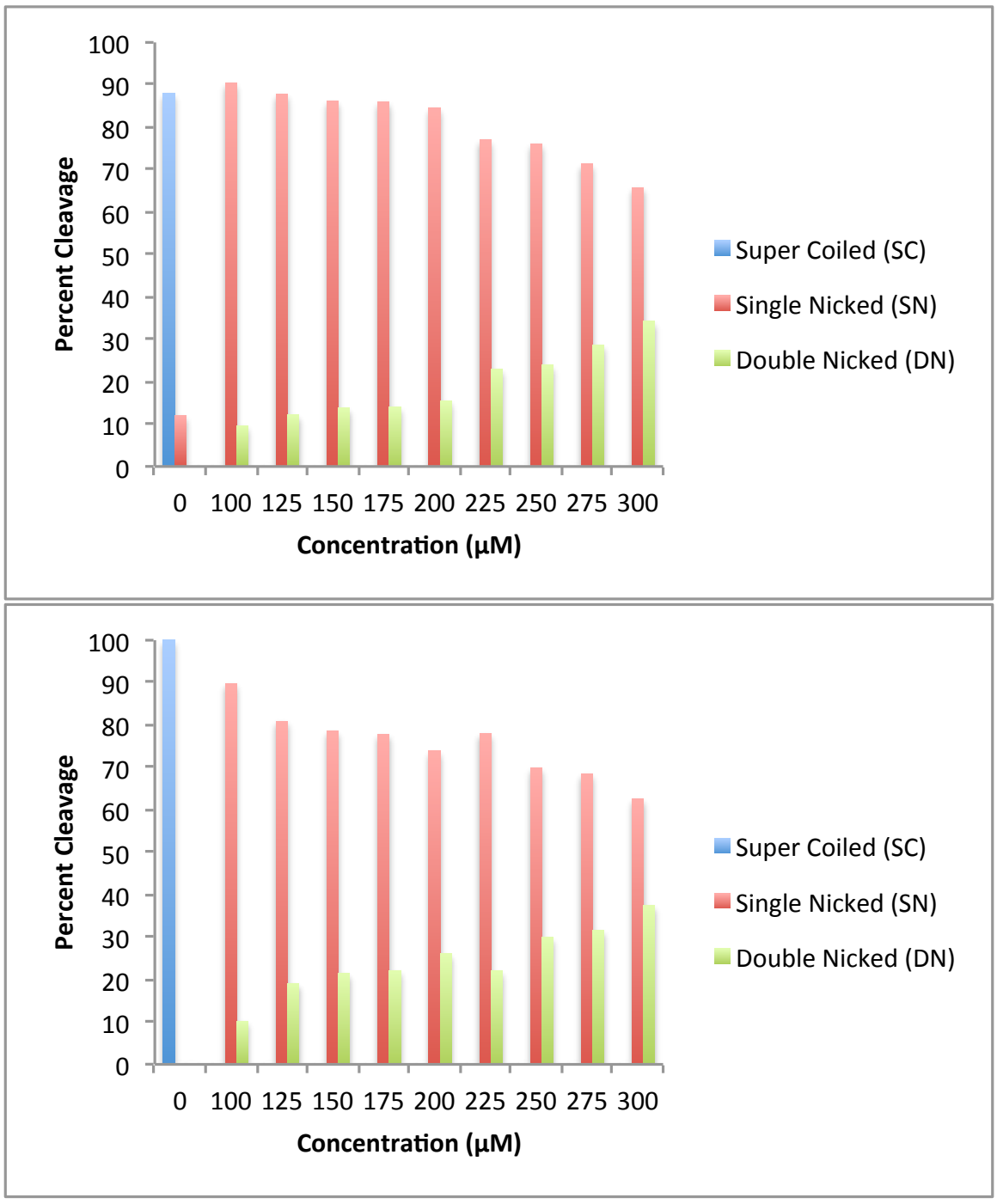


**Figure 11.** Relative percentages of DNA forms for DMSO mechanistic studies. Complex **1** (top) complex **2** (bottom).

The role of ROS in the mechanism indicated that both complexes react via an oxidative mechanism Based on the mechanistic studies it was concluded that $^1O_2$ plays an important mechanistic role in the cleavage of DNA by complexes **1** and **2**, but that •OH does not play a role in either complex's mechanism of action. Since neither scavenger was able to completely inhibit nuclease activity, additional mechanistic studies need to be carried out to determine if other ROS, such as superoxide, are involved in the mechanism.

*3.4 DNA Binding Studies*

The exhibited nuclease activity of complexes **1** and **2** indicate that they interact with DNA. However, it is unclear what type of interaction(s) is (are) occurring. One of the goals of this project was to carry out DNA binding studies using ethidium bromide (EtBr) in order to determine if the complexes intercalate DNA. Compounds that exhibit DNA intercalation are able to insert themselves between the DNA bases. EtBr is a known DNA intercalating agent with a very strong binding affinity, with $K_{ds\text{-}DNA}$=130E10$^4$ $M^{-1}$ (the binding constant to double-stranded DNA).[28] One of the main reasons EtBr can be used in these types of studies is because the EtBr-DNA complex has a characteristic fluorescence.[29,30] In the presence of a reagent that can competitively intercalate into DNA a decrease in this fluorescence is observed because some of the EtBr is displaced from the DNA where bulk solvent quenches the florescence signal.[30,31] If a decrease in fluorescence is observed in the presence of complex within a solution containing EtBr and DNA then it can be concluded that the complex is an intercalating agent. Additionally, the amount of fluorescence quenching can be mathematically related to the complex's DNA binding constant ($K_{bind}$).

Solutions containing a constant concentration of EtBr and CT-DNA were prepared with a complex concentration range of 0-105 μM. However, both complex **1** and **2** formed a cloudy precipitate when added into the solution mixture. Since fluorescence data can only be collected with a clear solution, these studies are still inconclusive. Some preliminary work has been conducted which indicates that increasing the overall percentage of DMF in these solutions may prevent the formation of precipitate. Initial measurements using complex **2** with solution containing 30% DMF using an incubation time of 30 min did not show any discernable trend. Further studies are needed to determine if increasing the incubation time would yield different results, because the initial incubation time used may not have been sufficient for complete binding to occur.

*3.5 Protein Binding Studies*

Another important aspect to consider when designing chemotherapeutic agents is their ability to be transported throughout the body because they must reach the site of cancer in order to be effective. Human Serum Albumin (HSA) is the most abundant protein in human blood serum.[32] Therefore, binding of potential chemotherapeutic agents to this protein is of interest when trying to determine if a compound has the potential to be circulated throughout the body. Additionally, some studies have found that serum proteins accumulate in tumor tissue so binding these proteins may help the complex aggregate in the desired target region.[33] Bovine serum albumin is an analog to HSA that is found in bovine.[34] Compounds' binding constants to BSA have also been related to their distribution throughout, and excretion from, the body.[35] BSA has a characteristic

fluorescence when it is free in solution and this fluorescence decreases when it is bound to something that decreases the exposure of its tryptophan residues.[32] Similarly to the EtBr studies previously described, the amount of fluorescence quenching can be measured and used to determine a binding constant. In order to extract the binding constant of complex **1,** solutions were prepared with varying concentration of complex in the presence of a constant concentration of BSA and fluorescence measurements were taken. The fluorescence measurements showed that complex **1** is capable of fluorescing in the observed region in the absence of BSA. Figure 12 shows the fluorescence of complex **1** in buffer with 30% DMF at concentrations from 0-110 μM with an excitation wavelength 280 nm over a range of 290-450 nm. The inherent fluorescence of the complex interfered with attempts to measure a change in the fluorescence of BSA at these wavelengths. Further studies should be carried out to determine if a different excitation wavelength can be used and to determine if complex **2** exhibits the same fluorescence.

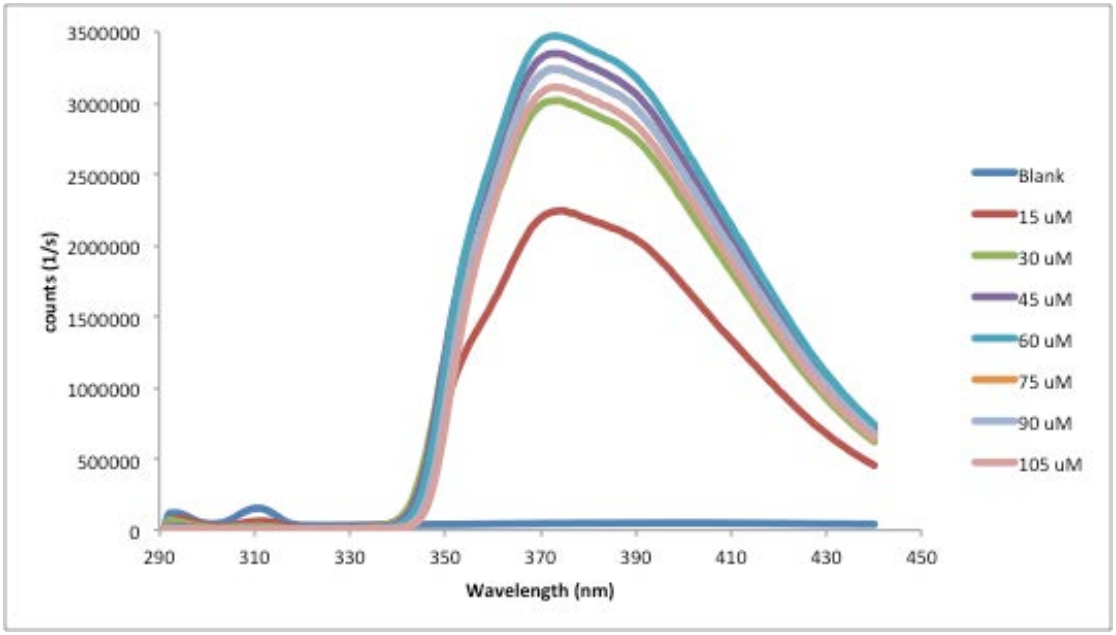


**Figure 12**. Emission spectra of complex **1** in buffer with 30% DMF.

*3.6 Conclusions*

The complexes $Cu(PyOMe(oBt))Cl_2$ (**1**), $[Cu(PyOMe(oBt)_2(NO_3)]NO_3$ (**2**), and $[Cu_2(PyOMe(en))(PyOMe(enH_2)_2](NO_3)_4$ (**3**) were successfully synthesized and characterized. The observed structural differences between complex **1** and **2** were a result of varying the starting metal. Complex **3** demonstrated an interesting ability to self-hydrolyze, however it is still uncertain if the extent of this hydrolysis of the ligand backbone is consistent in each synthetic reaction. It has been demonstrated that complexes **1** and **2** exhibit concentration dependent nuclease activity. Additionally, **2** was able to act as a more efficient nuclease compared to complex **1**. The differences in reactivity can likely be attributed to the complexes differing overall charges. Complex **2** has an overall positive charge, whereas complex **1** is neutral. Mechanistic studies showed that both complex **1** and **2** cleave DNA via an oxidative mechanism and $^1O_2$ plays a key role in this mechanism. Additionally, these studies showed that •OH does not play a role in DNA cleavage by these complexes. There are several additional studies that are needed in order to fully characterize the biological activity of these complexes and make subsequent comparisons. These studies include additional mechanistic studies of other ROS, DNA intercalation studies using EtBr, and BSA binding studies.

## References


1. American Cancer Society, *Cancer Facts & Figures,* 2012
2. Varmus, Harold, and Robert Weinberg. *Genes and the Biology of cancer*. New York: Scientific American Library, 1993. Print
3. Almeida, Craig, and Sheila Barry. "The Basics of Cancer." Trans. Array *Cancer: Basic Science and Clinical Aspects*. . 1st. Massachusetts: Wiley-Blackwell, 2012. 1-23. Print.
4. Potten, C. S., and James W. Wilson. *Apoptosis: the life and death of cells*. Cambridge New York: Cambridge University Press, 2004. Print.
5. Green, Douglas R. *Means to an end: apoptosis and other cell death mechanisms*. Cold Spring Harbor, N.Y: Cold Spring Harbor Laboratory Press, 2011. Print.
6. Lowe, S. W. Apoptosis in cancer. Carcinogenesis (New York) 21.3 Mar 2000: 485-495. Oxford University Press. 24 Sep 2013.
7. Kasibhatla, S. Why target apoptosis in cancer treatment?. Molecular cancer therapeutics 2.6 2003: 573. American Association for Cancer Research. 24 Sep 2013.
8. Brown, J. Martin, and Laura D. Attardi. "The role of apoptosis in cancer development and treatment response." *Nature Reviews Cancer* 5.3 (2005): 231-237.
9. Almeida, Craig, and Sheila Barry. "Cancer Treatment Modalities." Trans. Array *Cancer: Basic Science and Clinical Aspects*. . 1st. Massachusetts: Wiley-Blackwell, 2012. 1-23. Print.
10. Alderden, Rebecca, Matthew Hall, and Trevor Hambley. "The Discovery and Development of Cisplatin."*Journal of Chemical Education*. 85.5 (2006): 728. Print.
11. Eastman, Alan. "The Mechanism of Action of Cisplatin: From Adducts to Apoptosis." Trans. Array*Cisplatin: Chemistry and Biochemistry of a Leading Anticancer Drug*. Wiley-VCH, 1999. Print.
12. Malinge, Jean-Marc, and Marc Leng. "Interstrand Cross-Links in Cisplatin- or Transplatin-Modified DNA." Trans. Array *Cisplatin: Chemistry and Biochemistry of a Leading Anticancer Drug*. Wiley-VCH, 1999. Print.
13. Cepeda, Victoria, et al. "Biochemical mechanisms of cisplatin cytotoxicity."*Anti-Cancer Agents in Medicinal Chemistry (Formerly Current Medicinal Chemistry-Anti-Cancer Agents)* 7.1 (2007): 3-18.
14. O'Dwyer, Peter, James Stevenson, and Steven Johnson. "Clinical Status of Cisplatin, Carboplatin, and Other Platinum-Based Antitumor Drugs." Trans. Array*Cisplatin: Chemistry and Biochemistry of a Leading Anticancer Drug*. Wiley-VCH, 1999. Print.
15. Alcindor, T., and N. Beauger. "Oxaliplatin: a review in the era of molecularly targeted therapy." *Current oncology* 18.1 (2011): 18.
16. Xiaoyong Wang and Zijian Guo. *"Targeting and delivery of platinum-based anticancer drugs" Chem Soc Rev.* 2013, 202-224.
17. Marzano, Cristina, et al. "Copper complexes as anticancer agents." *Anti-Cancer Agents in Medicinal Chemistry* 9.2 (2009): 185-211.
18. Gupte, Anshul, and Russell J. Mumper. "Elevated copper and oxidative stress in cancer cells as a target for cancer treatment." *Cancer treatment reviews*35.1 (2009): 32-46.
19. Lin, Han. B.S. Thesis, Union College, 2013
20. Foreman, David. B.S. Thesis, Union College, 2013
21. Fox K. "*Fox Research Laboratory Protocols*", Union College, Schenectady, NY August 2013.
22. Steiner, Ramsey A., et al. "Synthesis, characterization, crystal structures and biological activity of set of Cu (II) benzothiazole complexes: Artificial nucleases with cytotoxic activities." *Journal of inorganic biochemistry* 137 (2014): 1-11.
23. Rajendiran, Venugopal, et al. "Mixed-ligand copper (II)-phenolate complexes: effect of coligand on enhanced DNA and protein binding, DNA cleavage, and anticancer activity." *Inorganic chemistry* 46.20 (2007): 8208-8221.
24. Kirin, Srecko I., et al. "Synthesis, structure and comparison of the DNA cleavage ability of metal complexes M (II) L with the N-(2-ethoxyethanol)-bis (2-picolyl) amine ligand L (M= Co, Ni, Cu and Zn)." *Dalton Transactions* 8 (2004): 1201-1207.
25. Detmer, Charles A., Filomena V. Pamatong, and Jeffrey R. Bocarsly. "Nonrandom double strand cleavage of DNA by a monofunctional metal complex: mechanistic studies." *Inorganic Chemistry* 35.21 (1996): 6292-6298.

**26.** Loganathan, Rangasamy, et al. "Mixed ligand copper (II) complexes of N, N-bis (benzimidazol-2-ylmethyl) amine (BBA) with diimine co-ligands: efficient chemical nuclease and protease activities and cytotoxicity." *Inorganic chemistry* 51.10 (2012): 5512-5532.

**27.** Ghosh, Kaushik, et al. "Nuclease activity via self-activation and anticancer activity of a mononuclear copper (II) complex: novel role of the tertiary butyl group in the ligand frame." *Inorganic chemistry* 51.6 (2012): 3343-3345.

**28.** Vardevanyan, P. O., et al. "The binding of ethidium bromide with DNA: interaction with single-and double-stranded structures." *Experimental and Molecular medicine* 35.6 (2003): 527-533.

**29.** Reinhardt, Christian G., and Thomas R. Krugh. "A comparative study of ethidium bromide complexes with dinucleotides and DNA: direct evidence for intercalation and nucleic acid sequence preferences." *Biochemistry* 17.23 (1978): 4845-4854.

**30.** O'Connor, Mark, et al. "Copper (II) complexes of salicylic acid combining superoxide dismutase mimetic properties with DNA binding and cleaving capabilities display promising chemotherapeutic potential with fast acting in vitro cytotoxicity against cisplatin sensitive and resistant cancer cell lines."*Journal of medicinal chemistry* 55.5 (2012): 1957-1968.

**31.** Saha, Biswarup, et al. "DNA Binding Ability and Hydrogen Peroxide Induced Nuclease Activity of a Novel Cu (II) Complex with Malonate as the Primary Ligand and Protonated 2-Amino-4-picoline as the Counterion†." *The Journal of Physical Chemistry B* 114.17 (2010): 5851-5861.

**32.** Stanyon, Helen F., and John H. Viles. "Human Serum Albumin Can Regulate Amyloid-β Peptide Fiber Growth in the Brain Interstitium IMPLICATIONS FOR ALZHEIMER DISEASE." *Journal of Biological Chemistry* 287.33 (2012): 28163-28168.

**33.** Kratz, Felix, et al. "A novel macromolecular prodrug concept exploiting endogenous serum albumin as a drug carrier for cancer chemotherapy." *Journal of medicinal chemistry* 43.7 (2000):1253-1256.

**34.** Bradshaw, Ralph A., and Theodore Peters. "The amino acid sequence of peptide (1–24) of rat and human serum albumins." *Journal of Biological Chemistry* 244.20 (1969): 5582-5589.

**35.** Chi, Zhenxing, et al. "Binding of oxytetracycline to bovine serum albumin: spectroscopic and molecular modeling investigations." Journal of Agricultural and Food Chemistry 58.18 (2010): 10262-10269.

**Acknowledgements**

I would like to thank Professor Laurie Tyler for all of her contagious enthusiasm, guidance and support with this project, as well as all of her guidance outside of the lab. Additionally, I would like to thank Professor Kristin Fox for all of her help with the biological studies. I would also like to thank the Scortino Summer Research Fellowship for funding my summer research and the Union College Internal Education Fund for funding my research during this academic year. Finally, I would like to thank the Union College Chemistry Department, my lab partner Courtney Elwell, and our X-ray crystallographer Prof. Joseph Tanski.

## Appendix

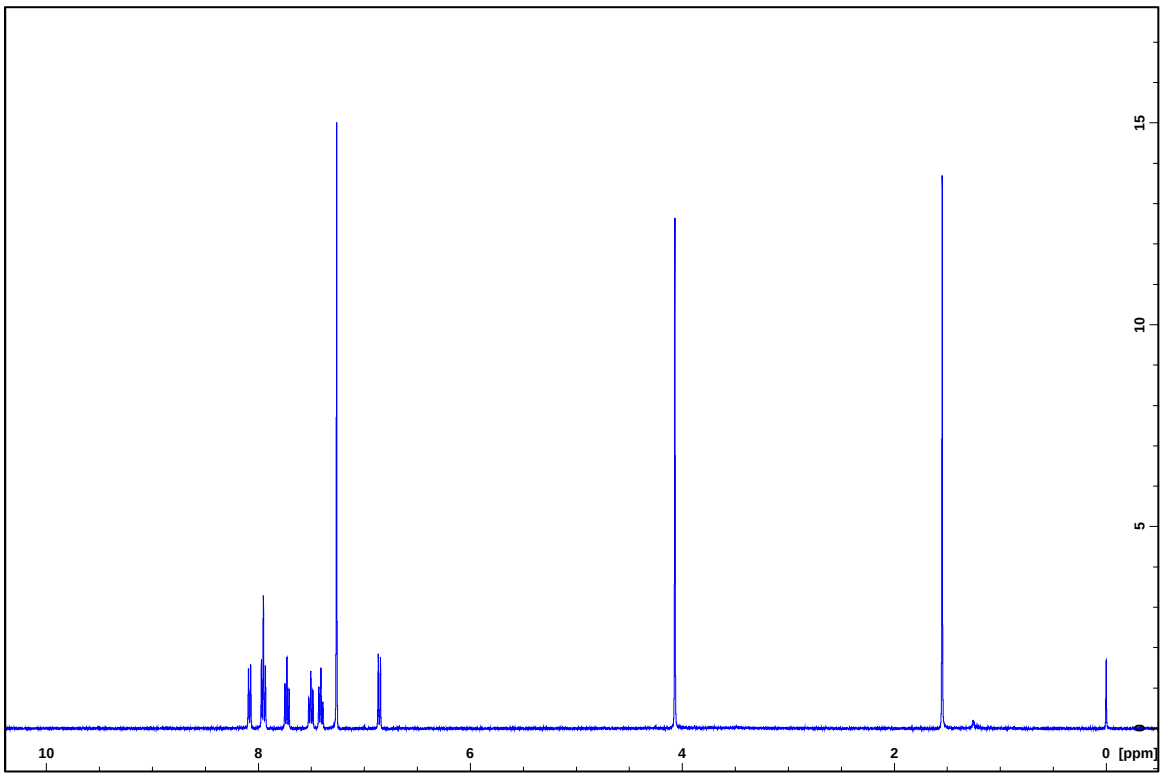


**Appendix 1**. $^{1}H$ NMR spectrum of PyOMe(oBt) in $CDCl_3$.

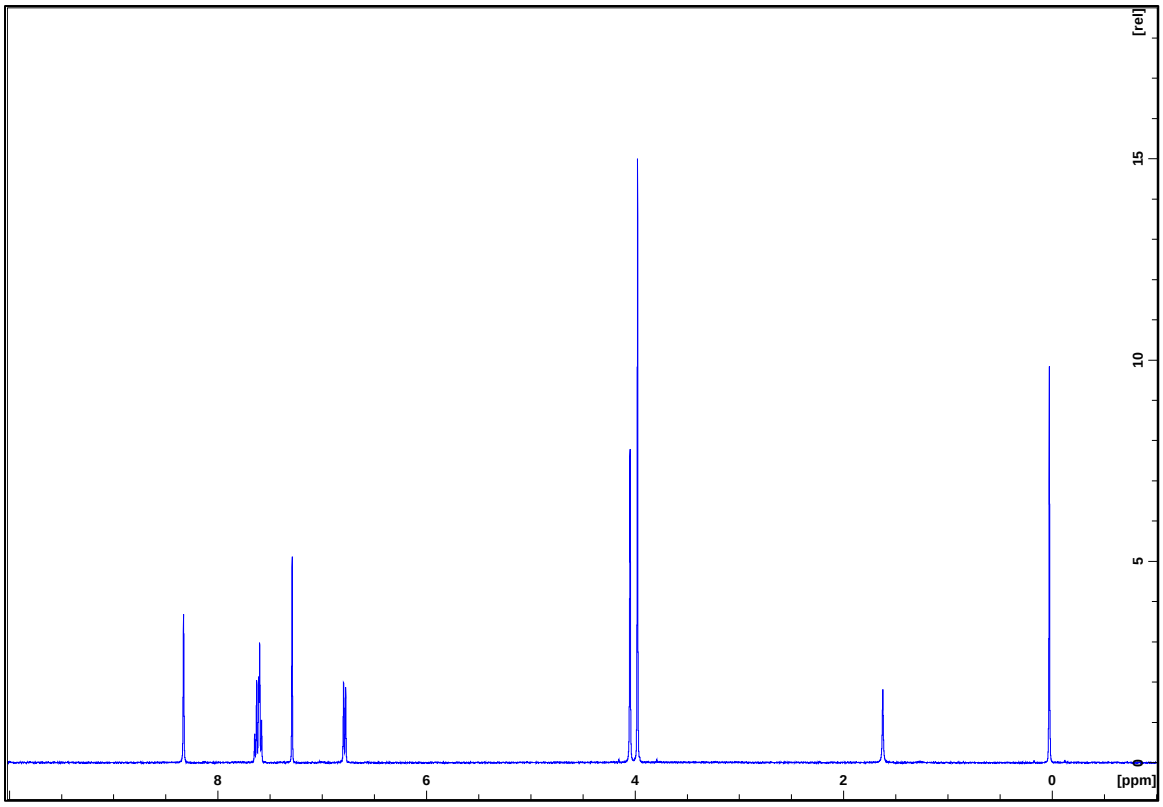


**Appendix 2**. $^{1}H$ NMR spectrum of PyOMe(en) in $CDCl_3$.

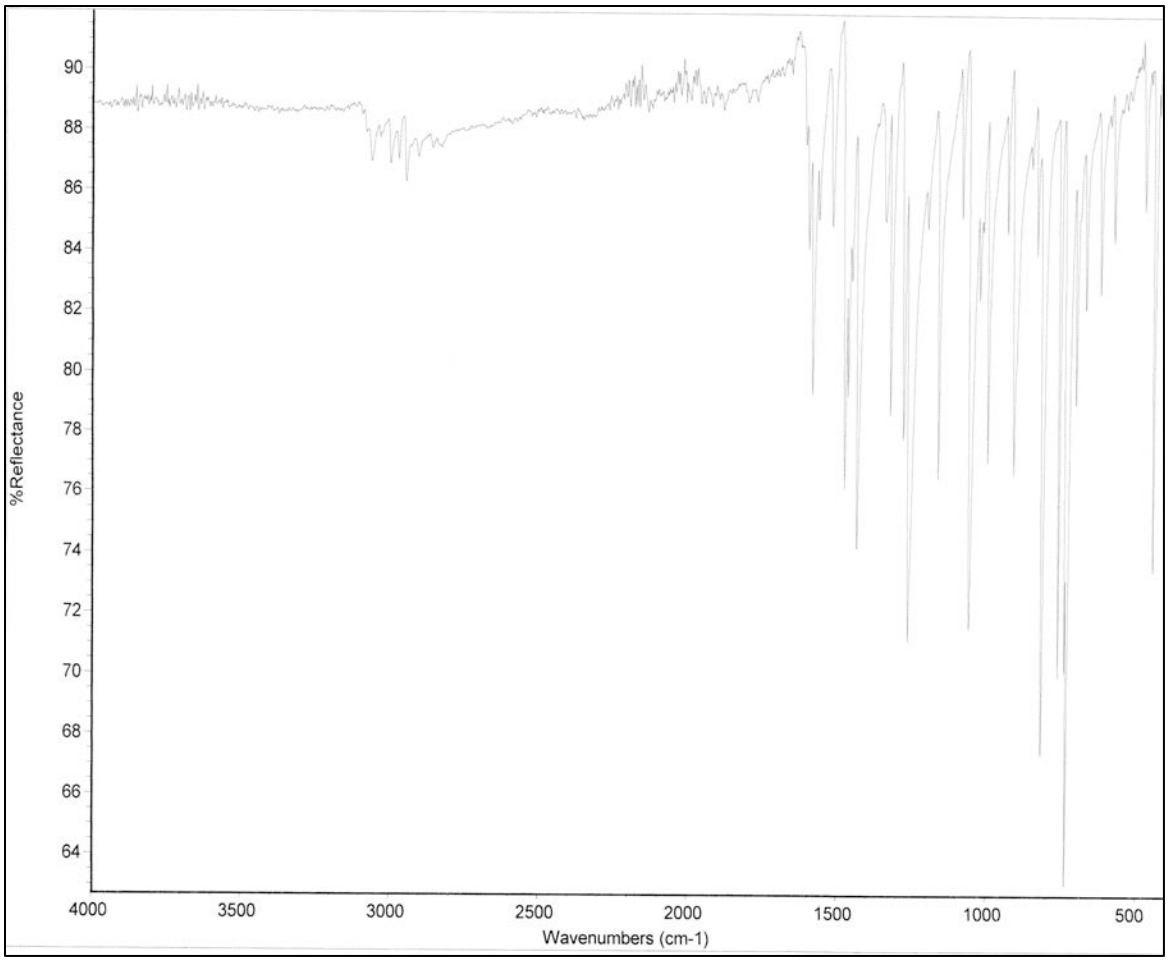


**Appendix 3**. IR spectrum of PyOMe(oBt) ligand.

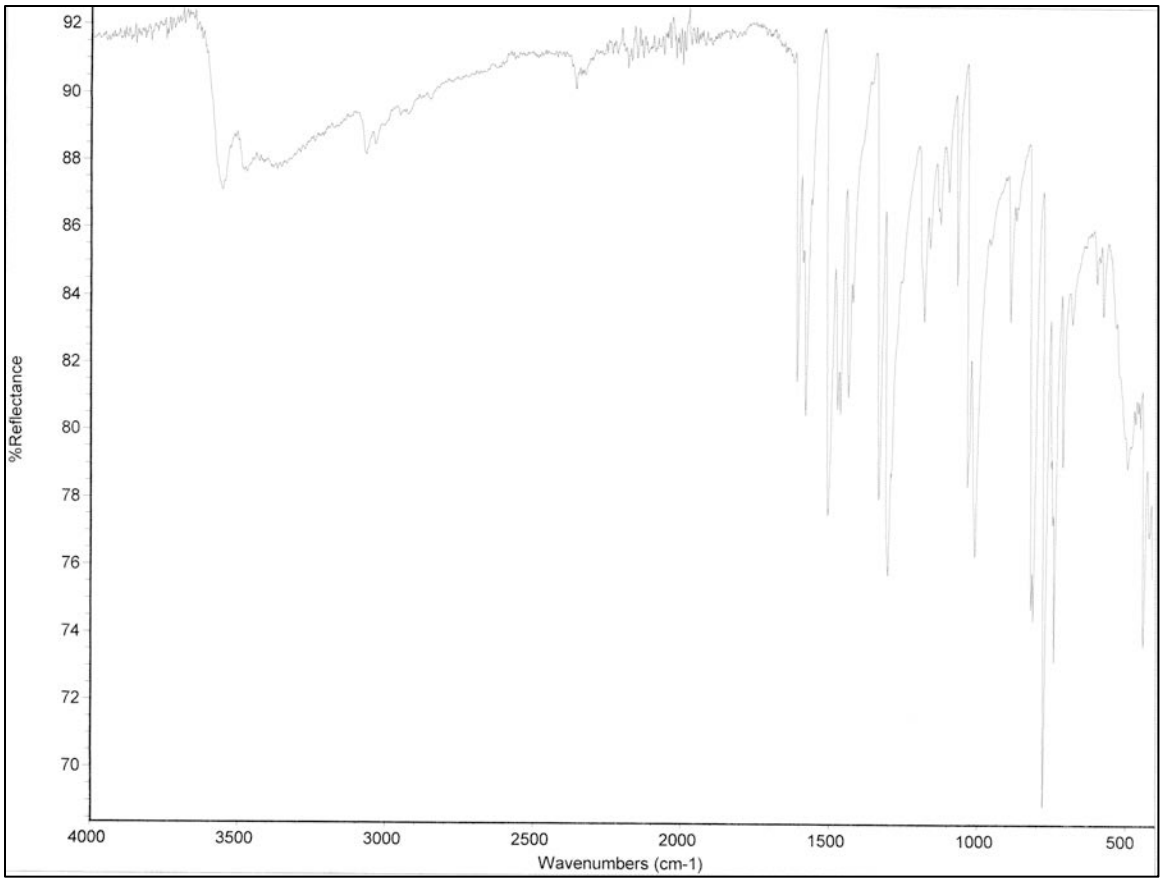


**Appendix 4.** IR spectrum of Cu(PyOMe(oBt))$Cl_2$.

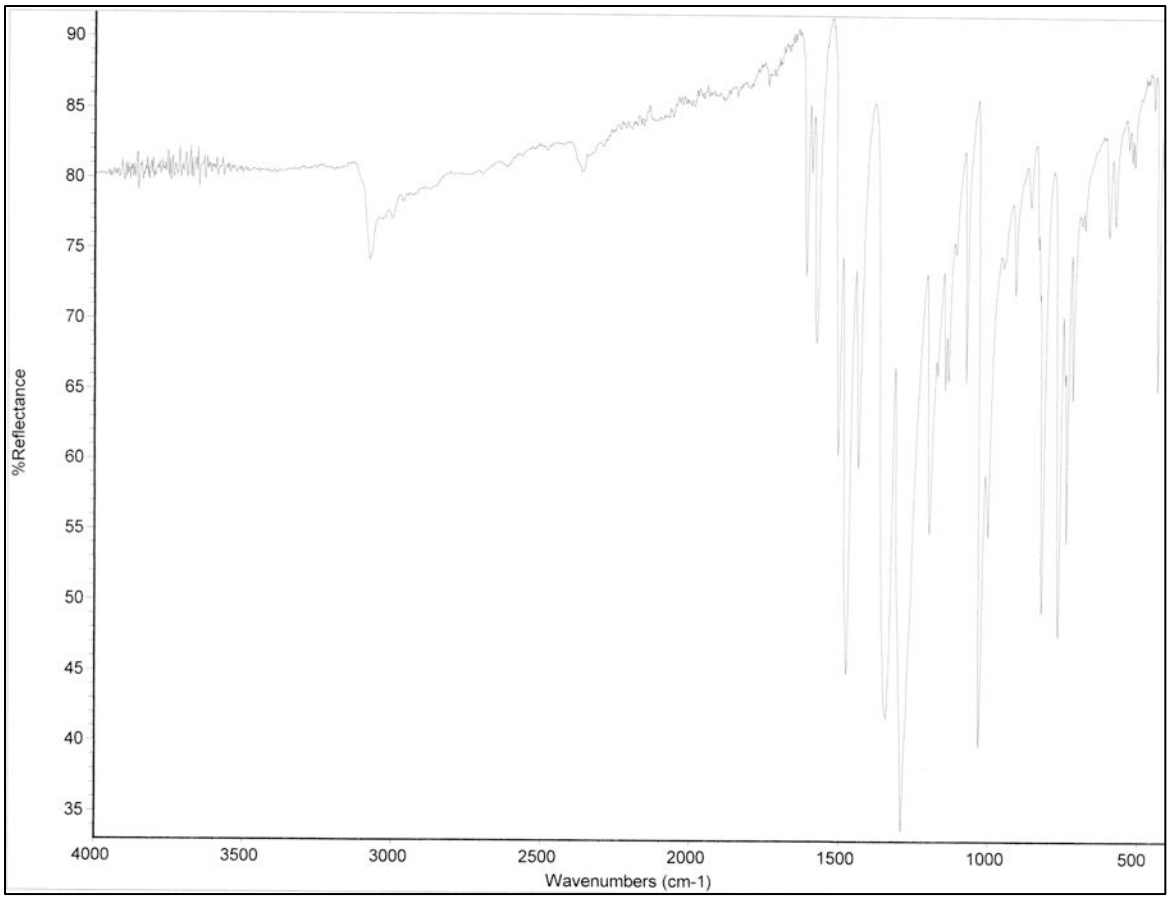


**Appendix 5.** IR spectrum of $[Cu(PyOMe(oBt)_2(NO_3)]NO_3$.

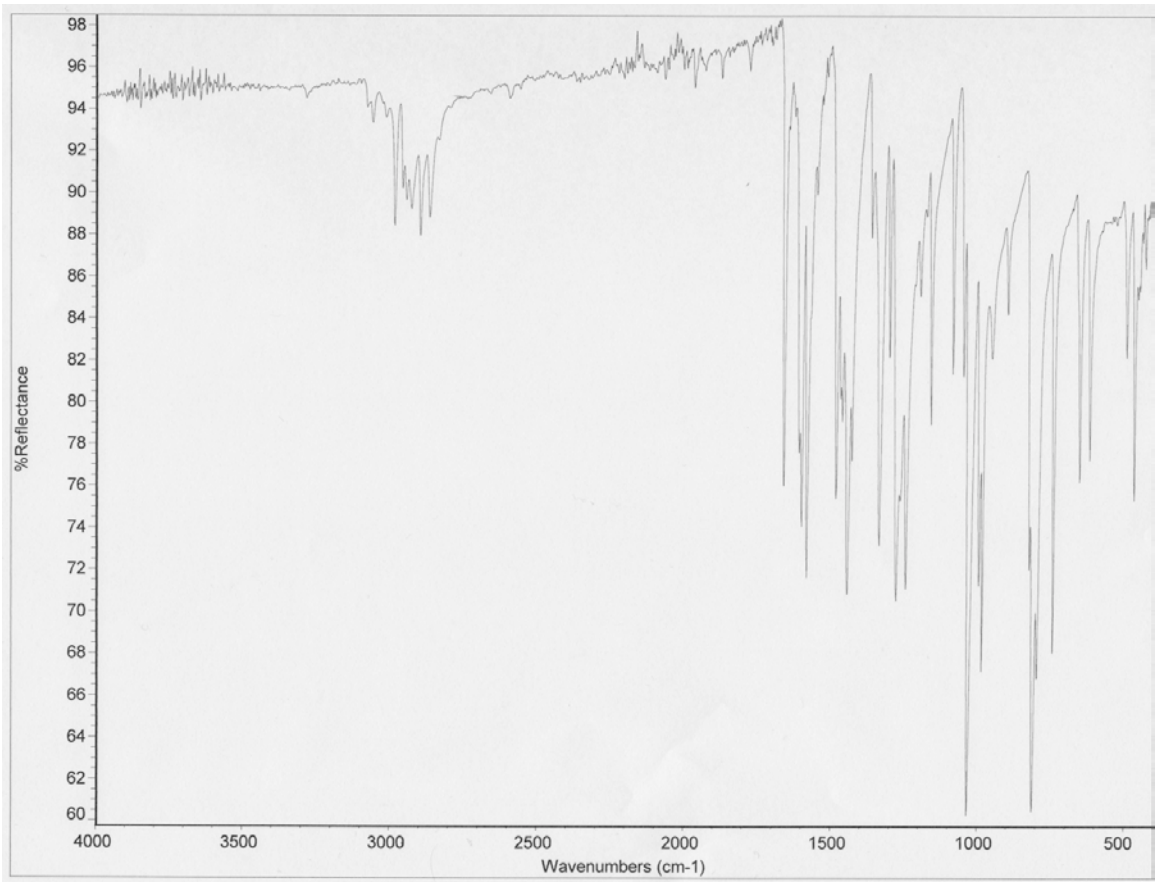


**Appendix 6.** IR spectrum of PyOMe(en).

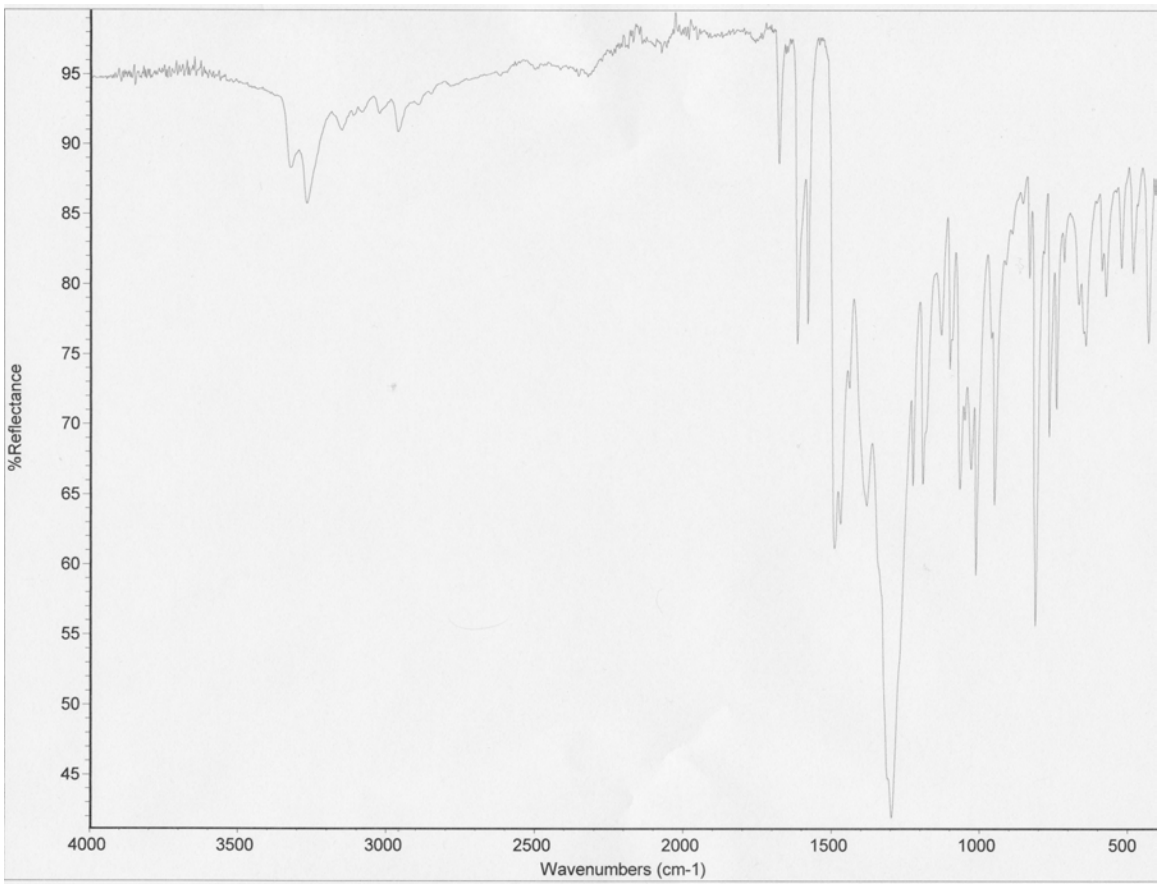


**Appendix 7.** IR spectrum of $[Cu_2(PyOMe(en))(PyOMe(enH_2)_2](NO_3)_4$.